Molecular Therapy
Methods & Clinical Development
Original Article

A High-Throughput Method for Characterizing Novel Chimeric Antigen Receptors in Jurkat Cells

Darin Bloemberg,[2] Tina Nguyen,[2] Susanne MacLean,[2] Ahmed Zafer,[2] Christine Gadoury,[1] Komal Gurnani,[2] Anindita Chattopadhyay,[2] Josée Ash,[1] Julie Lippens,[1] Doreen Harcus,[1] Martine Pagé,[1] Annie Fortin,[1] Robert A. Pon,[2] Rénald Gilbert,[1,3] Anne Marcil,[1] Risini D. Weeratna,[2] and Scott McComb[2,4]

[1]Human Health Therapeutics Research Centre, National Research Council Canada, Montréal, QC H4P 2R2, Canada; [2]Human Health Therapeutics Research Centre, National Research Council Canada, Ottawa, ON K1A 0R6, Canada; [3]Department of Bioengineering, McGill University, Montréal, QC H3A 0E9, Canada; [4]Department of Biochemistry, Microbiology, and Immunology, Faculty of Medicine, University of Ottawa, Ottawa, ON K1H 8M5, Canada

Chimeric antigen receptor (CAR) development involves extensive empirical characterization of antigen-binding domain (ABD)/CAR constructs for clinical suitability. Here, we present a cost-efficient and rapid method for evaluating CARs in human Jurkat T cells. Using a modular CAR plasmid, a highly efficient ABD cloning strategy, plasmid electroporation, short-term co-culture, and flow-cytometric detection of CD69, this assay (referred to as CAR-J) evaluates sensitivity and specificity for ABDs. Assessing 16 novel anti-CD22 single-chain variable fragments derived from mouse monoclonal antibodies, CAR-J stratified constructs by response magnitude to CD22-expressing target cells. We also characterized 5 novel anti-EGFRvIII CARs for preclinical development, identifying candidates with varying tonic and target-specific activation characteristics. When evaluated in primary human T cells, tonic/auto-activating (without target cells) EGFRvIII-CARs induced target-independent proliferation, differentiation toward an effector phenotype, elevated activity against EGFRvIII-negative cells, and progressive loss of target-specific response upon *in vitro* re-challenge. These EGFRvIII CAR-T cells also showed anti-tumor activity in xenografted mice. In summary, CAR-J represents a straightforward method for high-throughput assessment of CAR constructs as genuine cell-associated antigen receptors that is particularly useful for generating large specificity datasets as well as potential downstream CAR optimization.

INTRODUCTION

Genetically engineering the immune system shows broad promise for treating cancer, particularly using chimeric antigen receptor (CAR)-T cells. Adoptive cell therapy using CD19-targeted CAR-T cells has demonstrated remarkable efficacy in patients with chemotherapy-resistant and relapsed hematological malignancies, where clinical trials have shown response rates sometimes exceeding 90%.[1–3] Partly due to its success in treating leukemia, trials involving CAR-T cell targeting numerous cancer antigens—including BCMA, CD20, CD22, CD30, CD138, c-met, EGFRvIII, FAB, GD2, HER2, WT1, PSMA, interleukin (IL)-13R-α2, NY-ESO1, EGFR, and CD133—are ongoing, with many more target antigens under development.[4–6]

CAR molecules have four main functional regions: (1) an extracellular antigen-binding domain (ABD), normally a single-chain variable fragment (scFv) derived from monoclonal antibodies (MAbs) isolated from mouse or other species, (2) a spacer and/or hinge domain, (3) a transmembrane domain, and (4) an intracellular activation domain[7] (Figures 1A and 1B). While some antibody properties such as affinity, specificity, and internalization may be useful for predicting which ABDs represent functional CARs, they must ultimately be tested in the context of an antigen receptor to assess properties such as surface expression, auto-activation, and effector cell function.[8,9] Here, we outline a high-throughput, cost-effective, and efficient method for designing, cloning, and screening CAR constructs using Jurkat cells. This advancement is anticipated to accelerate the discovery and improve the quality of candidate CAR-T cell therapies for future clinical applications.

RESULTS

pSLCAR: A Modular CAR Vector Suitable for High-Throughput Screening

To enable high-throughput CAR recombination and screening, we generated modular simple lentiviral plasmids: pSLCAR and pSLCAR-CD19 (Figure 1C). pSLCAR-CD19 contains type-IIs restriction sites to allow efficient and scarless exchange of the ABD gene sequence using a single-tube restriction/ligation reaction. This minimizes DNA synthesis requirements, allowing high-speed and potentially highly automated construct screening. When delivered into mammalian cells, pSLCAR-CD19 expresses an anti-CD19-CD28-CD3ζ CAR (based on the FMC63-CD28-CD3ζ CAR; GenBank: HM852952.1)[10] using the EF1α-short promoter (EFS). A P2A ribosomal self-skipping sequence separates this CAR from an EGFP marker, thereby allowing fluorescent detection of CAR-expressing cells. 3rd-generation lentiviral elements were incorporated in the

Received 6 December 2019; accepted 27 January 2020;
https://doi.org/10.1016/j.omtm.2020.01.012.

Correspondence: Scott McComb, Human Health Therapeutics Research Centre, National Research Council Canada, 1200 Montreal Road (M54), Ottawa ON, Canada, K1A 0R6.
E-mail: scott.mccomb@nrc-cnrc.gc.ca

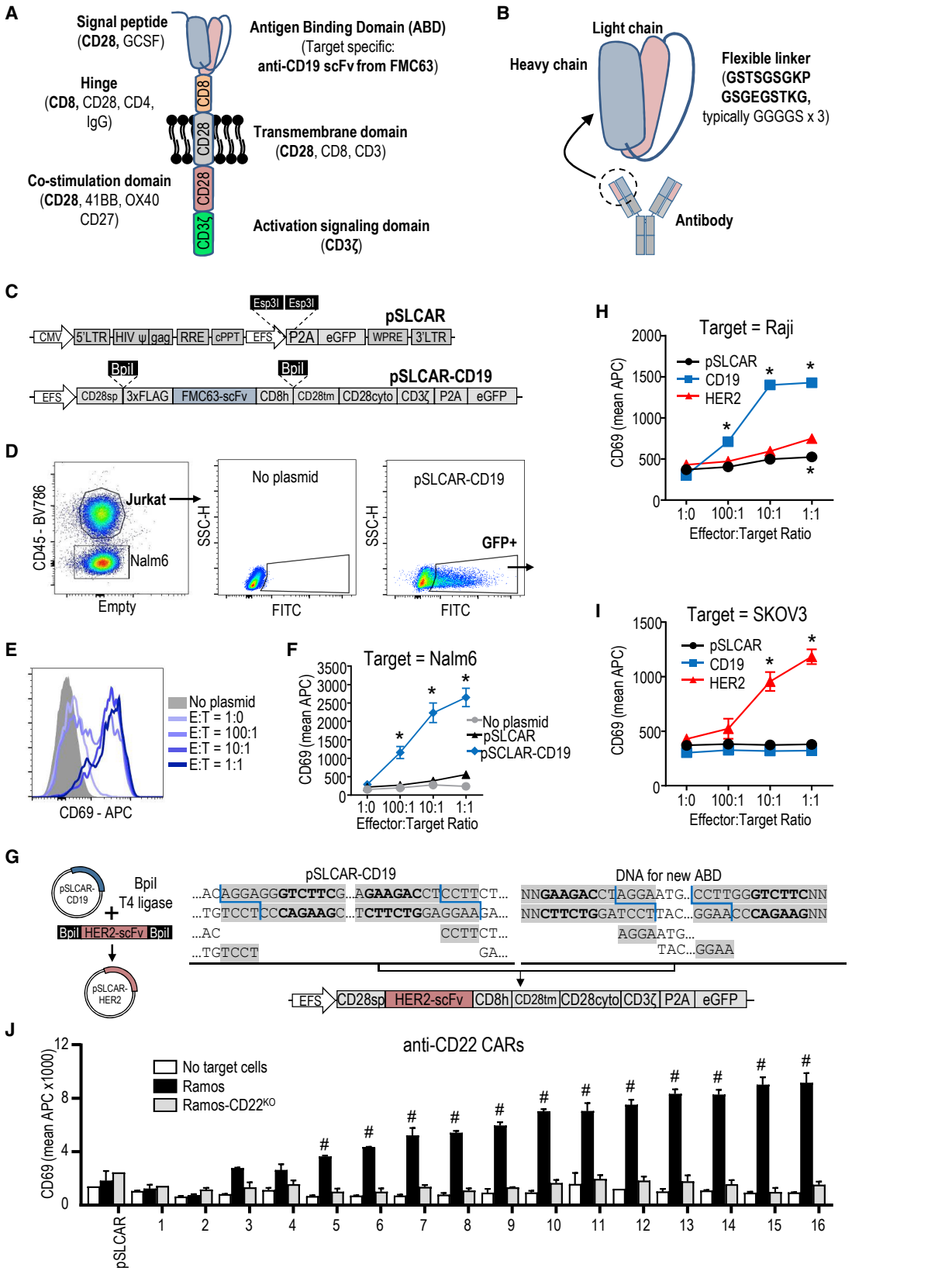

(legend on next page)

transfer plasmid to enable their use in both transient expression assays and generating cells with stable CAR expression in downstream experiments (Figure 1C).

Using Jurkat Cells to Detect CAR-Induced T Cell Activation: CAR-J

Jurkat cells are an immortal human leukemic T cell line[11] widely used to examine T cell activation and signaling mechanisms.[12] Although Jurkat cells do not secrete the entire cytokine repertoire of primary T cells and lack significant cytolytic activity, they do produce IL-2 and upregulate CD69 upon activation.[13,14] As cell-surface CD69 expression can be easily detected using fluorescent antibody staining, we pursued flow-cytometry-based CD69 measurement for assessing CAR-induced T cell activation, a strategy previously used by others conducting *in vitro* CAR testing.[15,16]

Briefly, Jurkat cells were electroporated with pSLCAR or pSLCAR-CD19, co-cultured with CD19-expressing target cells (Nalm6), stained with allophycocyanin (APC)-conjugated CD69 antibody, and analyzed using flow cytometry (Figure 1D; see Figure 7 for protocol diagram). Increasing target cell numbers progressively increased ($p < 0.05$) CD69 expression on GFP-positive Jurkat cells electroporated with pSLCAR-CD19 (Figures 1E and 1F). However, Jurkat cells with pSLCAR displayed minimal changes in CD69 (Figure 1F). Therefore, this CAR-Jurkat (CAR-J) assay adequately detects CAR-mediated activation in response to CD19-expressing cells.

We next evaluated whether CAR-J could distinguish between different CAR stimulatory elements (Figure S1). Importantly, removing all signaling and co-stimulatory domains eliminated CAR-J activation (Figures S1B and S1C). However, despite the known additive effects of co-stimulation on CAR-T cell function, constructs with different co-stimulatory domains (CD3ζ, CD28-CD3ζ, 41BB-CD3ζ, and CD28-41BB-CD3ζ) showed similar CD69 expression when cultured alongside Raji or Nalm6 cells (Figures S1B and S1C). Therefore, CAR-J may not be sufficiently sensitive to validate CAR signaling optimization strategies for specific scFv, such as those based on FMC63.

Simple ABD Swapping for Altering CAR-J Specificity

This modular CAR expression plasmid was designed to allow rapid and scarless ABD exchange. Here, an example of scFv swapping from anti-CD19 to anti-HER2 is described. The anti-HER2 scFv sequence derived from trastuzumab[17] was downloaded from the Protein Data Bank (PDB: 1N8Z), and DNA was synthesized to include terminal linkers containing BpiI restriction cassettes with compatible cohesive ends (Figure 1G). To insert this new CAR sequence, a single-tube restriction digestion/ligation recombination reaction[18] was conducted using pSLCAR-CD19-CD28-CD3ζ, transformant clones were assessed using colony PCR, and plasmid construction was confirmed with sequencing.

Redirection of CAR specificity was assessed by electroporating pSLCAR-CD19 and pSLCAR-HER2 into Jurkat cells and co-culturing with Raji (CD19+/HER2−) or SKOV3 (CD19−/HER2+) cells. CD69 was increased ($p < 0.05$) in CD19-CAR-J compared to HER2-CAR-J and control cells upon encountering Raji cells, demonstrating antigen-specific activation (Figure 1H). Conversely, CD69 was increased ($p < 0.05$) in HER2-CAR-J compared to other groups when incubated with SKOV3 cells, indicating complete and specific re-targeting to HER2-expressing targets (Figure 1I). These results demonstrate that surface CD69 upregulation in CAR-J can identify target-specific CAR activity.

Screening CAR Candidates Using CAR-J

To illustrate CAR-J's capacity for conducting high-throughput screening, Jurkat cells were electroporated with one of 16 pSLCAR-CD28-CD3ζ plasmids containing anti-CD22 scFvs derived from novel mouse MAbs. After sequencing hybridoma clones, scFv gene fragments for the 16 antibodies were synthesized (heavy-chain variable region, $(GGGGS)_3$ linker, light-chain variable region) and inserted into pSLCAR-CD19-CD28-CD3ζ via single-pot restriction ligation as described earlier, and plasmid clones were confirmed via Sanger sequencing. While all 16 demonstrated specific binding as antibodies to purified antigen and cells (data not shown), 4 constructs did not significantly increase ($p > 0.05$) CD69 above levels in cells electroporated with pSLCAR when conducting CAR-J with Ramos target cells (Figure 1J). The remaining 12 caused activation that was highly stratified and specific, as CD69 responses were eliminated when using Ramos cells with CRISPR-mediated CD22 knockout (Figure 1J). Thus, CAR-J can be used to examine a large set of novel CAR molecules for varying antigen-specific responsiveness.

Utility of CAR-J in Pre-clinical CAR Development

To illustrate the utility of this system in further characterizing CAR molecules, we examined five novel CAR ABDs targeting the mutated EGFR receptor EGFRvIII[19] shown to specifically bind

Figure 1. Development of pSLCAR and CAR-J: A Modular CAR Plasmid and Screening Strategy

(A) Typical CAR structure with examples of commonly used domains. Bold type indicates specific domains in the CAR construct used here. (B) Single-chain variable fragment (scFv) structure, as utilized in many CAR constructs. (C) Functional regions of simple lentiviral CAR plasmid (pSLCAR) and CD19-targeting pSLCAR. (D–F) Proof-of-concept CAR-J assay. (D) Illustration of flow cytometry gating strategy, permitting detection of CAR-expressing cells with GFP. (E) CD69-APC expression on GFP-positive Jurkat cells electroporated with pSLCAR-CD19 incubated with Nalm6 cells at increasing ratios. (F) Dose-response of CAR-J response to Nalm6. (G) Depiction of scFv swapping strategy and BpiI restriction cassettes contained in pSLCAR-CD19 with gene design for DNA fragments. (H and I) CAR-J conducted with Jurkat cells electroporated with anti-CD19 and anti-HER2 CARs. Targets were Raji (H) and SKOV3 (I). (J) CAR-J conducted using CARs derived from 16 antibodies previously determined to specifically bind CD22. Results in (F), (H), (I), and (J) represent means ± SEM of 3 independent experiments (n = 3). Asterisks in (F), (H), and (I) represent significant difference ($p < 0.05$) between the indicated group and all other groups at individual ratios, calculated using one-way ANOVAs. Pound signs in (J) represent significant difference ($p < 0.05$) between the indicated group and pSLCAR control, calculated using one-way ANOVA.

purified EGFRvIII and cells expressing EGFRvIII as antibodies (Figure S2A). These antibodies and CARs were generated as described earlier for CD22.

We used the high-throughput approach illustrated in Figure 2A to assess these anti-EGFRvIII CARs. Briefly, Jurkat cells were electroporated, seeded in 96-well plates, and co-cultured with varying numbers of U87 or EGFRvIII-expressing U87-vIII cells. Of the five CARs, two (F260 and F263) caused significant and consistent auto-activation (tonic signaling), as indicated by significantly increased CD69 expression ($p < 0.05$) compared to pSLCAR-CD19 control in the absence of target cells (Figure 2B). This indicates that F260 and F263 would likely be unsuitable clinical constructs, as they would potentially induce killing of non-specific cells and/or lead to early T cell exhaustion. The remaining CARs (F265, F269, and F271) did not induce significant activation ($p > 0.05$) in the absence of target cells or when co-cultured with U87 cells (Figure 2B) and progressively increased Jurkat CD69 expression with increasing numbers of U87-vIII cells (Figure 2C). Although statistically significant differences are disguised by the complexity of these responses, differences between groups are apparent when viewed as changes from baseline (Figure S2B). Therefore, this straightforward analysis allowed us to quickly identify the relative tonic/auto-activating and antigen-specific response characteristics of novel CAR molecules.

Adapting CAR-J to Rapid Construct Screening

The efficiency and robustness of the cloning method described here allows this protocol to be adapted for more high-throughput rapid CAR screening. Instead of isolating individual transformants and sequencing those displaying successful cloning based on colony PCR, we tested growing transformed cells directly in liquid culture as a polyclonal product (Figure S6).

This strategy was assessed by inserting the five EGFRvIII-targeting scFvs into pSLCAR-CD19 with three different signaling domains (28-3ζ, BB-3ζ, and 3ζ) using both "rapid" and "complete" recombination protocols. We then conducted CAR-J assays with these 30 plasmid preparations against 3 target cell lines (Nalm6, MCF7, and U87-vIII) at a 1:1 Jurkat-to-target ratio; 2 control plasmids (targeting CD19 and HER2) were also included. Importantly, neither recombination protocol displayed remnant responsiveness to CD19-expressing Nalm6 cells (Figures 2D and 2E), indicating that the rapid protocol removed detectable pSLCAR-CD19 plasmid. Furthermore, similar auto-activation and non-specific activation were observed with F260 and F263 as before. To more easily assess these differences, we calculated a "CAR-J magnitude/specificity score." Importantly, this score was not different ($p > 0.05$) between recombination protocols at individual construct-scFv combinations or for compiled data (Figure 2F). However, this analysis indicated differences between constructs and signaling domains (in contrast to results with FMC63-derived CARs; Figure S1), where BB-3ζ constructs displayed higher ($p < 0.05$) scores than 28-3ζ and 3ζ, and F269 displayed higher ($p < 0.05$) scores than all other scFvs (Figure 2F). Overall, this demonstrates the possibility of adapting CAR-J to rapid and genuine high-throughput screening.

CAR-J Tonic Signaling Correlates to Target Independent CAR-T Cell Signaling and T Cell Differentiation

We next examined whether CAR-J could predict CAR signaling properties in primary human T cells. T cells from 4 human donors were transduced with pSLCAR-28-3ζ lentivirus expressing our novel EGFRvIII-CARs, and these CAR-T cells were evaluated for several phenotypic markers during *in vitro* expansion (Figures 3A and 3B). At the time points examined, we did not observe significant CD69 expression on primary T cells. However, 7 days after transduction, expression of CD25 (IL-2Rα subunit) on CAR-positive cells mirrored the CAR-J auto-activation data ($R^2 = 0.77$), indicating prolonged activation of F260/F263 CAR-T cells compared to non-transduced T cells and F265/F269/F271 CAR-T cells ($p < 0.05$) (Figures 3A, 3C, and 3D). Notably, the CAR-J magnitude/specificity score (Figure 2F) proved to be highly predictive in this comparison ($R^2 = 0.93$) (Figure 3E). We also examined differentiation phenotypes 15 days after CD3/CD28 pan-T cell activation (Figure 3B). Here, CD45RO and PD1, markers expressed on effector and exhausted T cells, respectively, were elevated in auto-activating F260 and F263 CAR-T cells. Similarly, these CAR-T cells displayed lower levels of CD45RA and CD27, markers associated with naive/memory T cell subsets (Figure 3B). Overall, these data indicate that tonic signaling assessment via CAR-J is predictive of tonic signaling in primary human CAR-T cells.

Tonic Signaling CARs Lead to Target-Agnostic Activity and CAR-T Cell Exhaustion

To examine CAR-T cell effector functions, we used automated live imaging of co-cultures involving EGFRvIII CAR-T cells (green fluorescence) and various cancer cell lines stably expressing nuclear-localized mKate2 (red fluorescence) (Figure 4A). When cultured alone, F263 CAR-T cells continued to expand autonomously (these experiments were initiated 10 days after initial T cell activation) relative to F269 CAR-T and mock T cells (Figures 4A and 4B). When co-cultured with U87-vIII cells, both F263 and F269 CAR-T cells expanded transiently (Figure 4A and 4C; Figures S3–S5; Videos S1, S2, and S3) and eliminated U87-vIII cells (Figures 4A and 4D; Figures S3–S5; Videos S1, S2, and S3), although this response was quicker and more robust for F263 than for F269. Strikingly, while EGFRvIII-negative cancer cell lines (MCF7, SKOV3, and Nalm6) expanded similarly when co-cultured alongside mock-transduced T cells or F269 CAR-T cells, they were consistently all eliminated by F263 CAR-T cells (Figures 4A and 4E–4H; Figures S3–S5; Videos S4, S5, and S6). Average data across 3 donors for U87-vIII and MCF7 growth during co-culture are presented in Figures 4I and 4J. This non-specific effector response suggests that auto-activation signaling in the CAR-J assay relevantly predicts human CAR-T cell function.

To assess the serial and longer term killing capacity of our EGFRvIII-CARs, we repeatedly co-cultured donor 4 EGFRvIII CAR-T cells alongside U87-vIII cells as an *in vitro* tumor re-challenge (Figure 5).

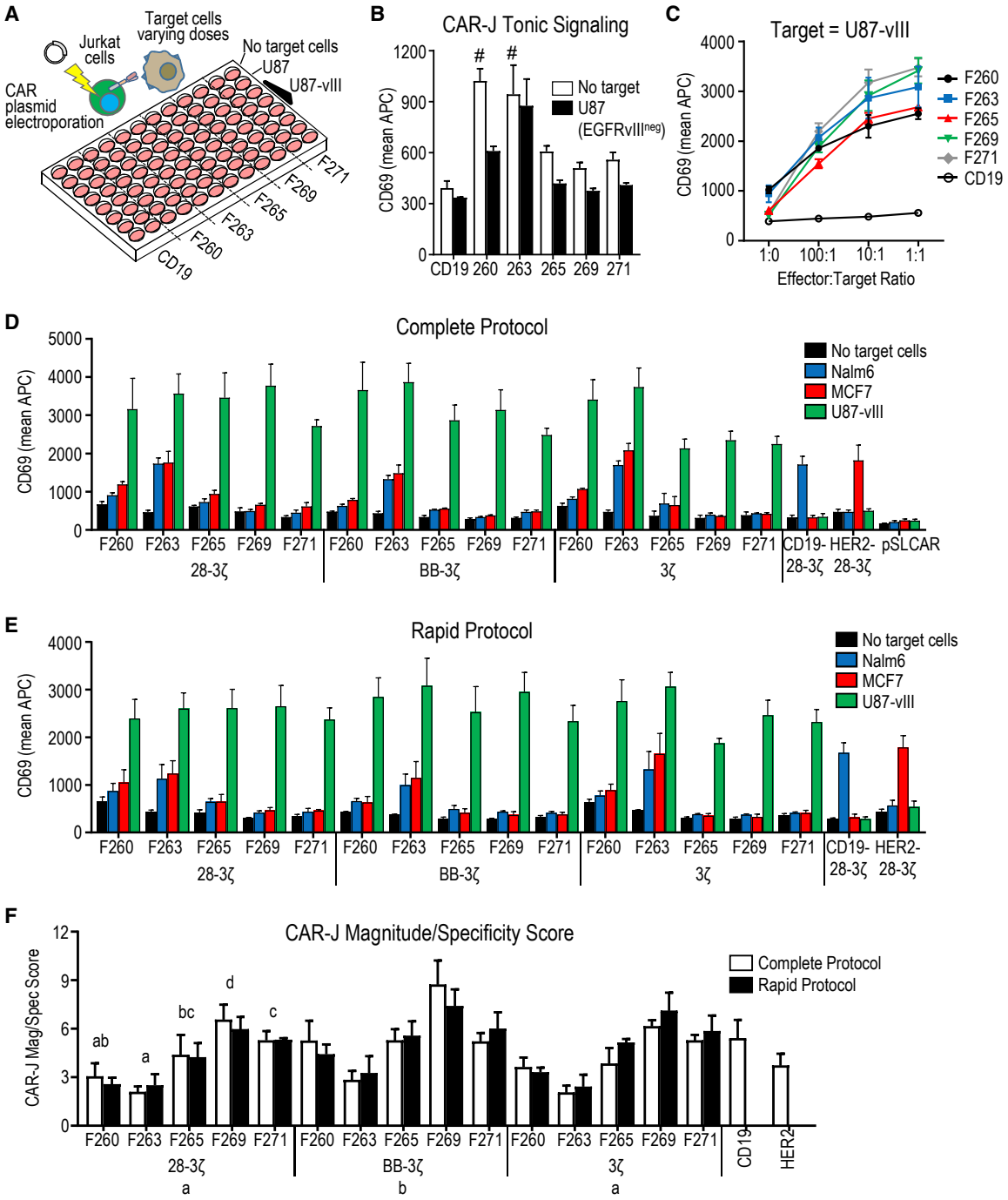

Figure 2. CAR-J Allows Short-Listing of Candidate scFv Sequences

(A) Overview of high-throughput CAR-J setup. (B) CAR-J tonic signaling (auto-activation) as indicated using flow cytometry assessment of surface CD69-APC expression when cultured alone (no target cells) or with EGFRvIII-negative U87 cells. (C) CAR-J dose-response activation when co-cultured alongside increasing numbers of U87-vIII cells. (D–F) Gene fragments encoding different anti-EGFRvIII scFvs were cloned into pSLCAR-CD19-28-3ζ, -BB-3ζ, or -3ζ. (D and E) CAR-J at a 1:1 Jurkat-to-target cell ratio using (D) cloned and sequenced (complete protocol) or (E) the polyclonal (rapid protocol) plasmid preparation. (F) These two approaches were compared using a CAR-J magnitude/specificity score (see Materials and Methods). Results represent means ± SEM of 3 independent experiments (n = 3). Pound signs in (B) represent significant difference ($p < 0.05$) between the indicated group and CD19 control, calculated using one-way ANOVA. In (F), protocols were not different (t test) when considered for individual construct-scFv combinations or when data were combined. A two-way ANOVA analysis of combined complete and rapid protocol data indicated main effects of construct and scFv, indicated with lowercase letters where groups with different letters are significantly different from each other.

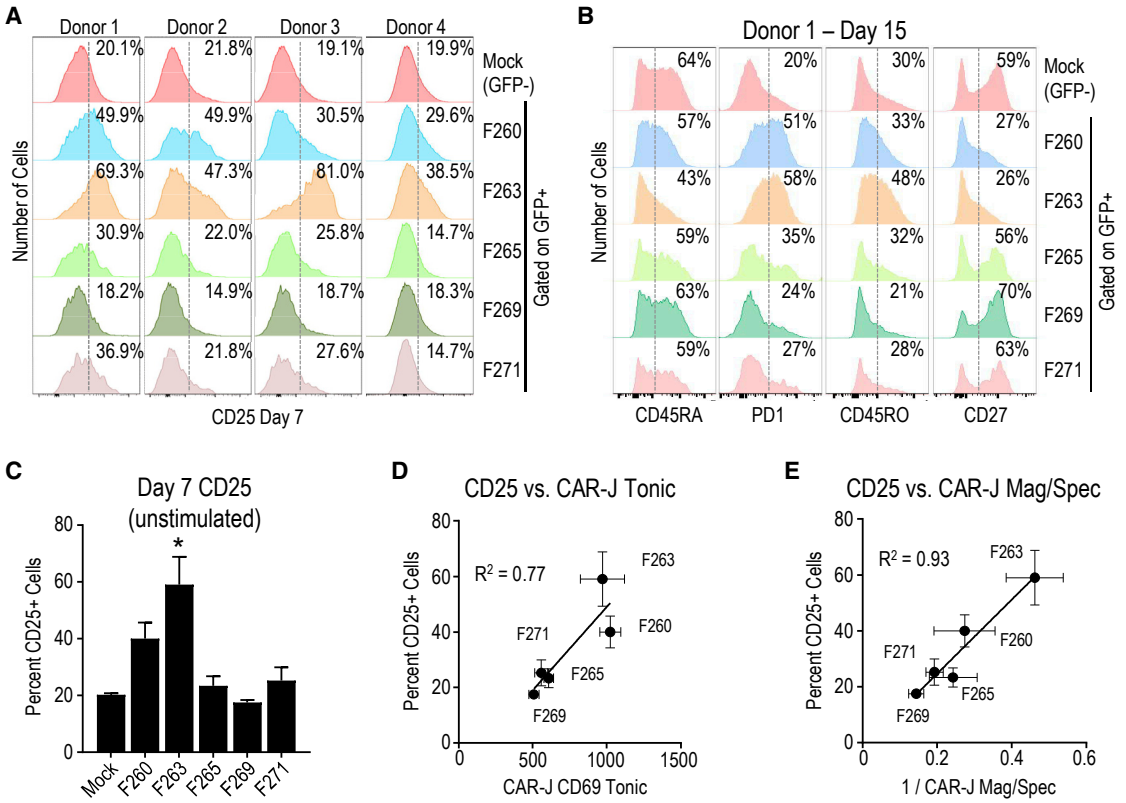

Figure 3. CAR-J Tonic Signaling Predicts Human Target-Independent CAR-T Cell Activity and Differentiation in Primary T Cells

Human CAR-T cells were generated from donor PBMCs via transduction with lentivirus produced from pSLCAR-EGFRvIII-CD28-CD3ζ. (A and B) Representative flow cytometry plots of T cell/CAR-T cell CD25 expression 7 days after lentiviral transduction (A) and other T cell phenotype markers on donor 1 15 days after transduction (B). (C) Quantification of CD25-positive cells in total (mock/untransduced T cells) or gated GFP-positive CAR-T cells (EGFRvIII-CAR-transduced cells) 7 days after transduction. (D) Correlation between day 7 CD25 and tonic CAR-J activation data from (C). (E) Similarly, the relationship between day 7 CD25 and the CAR-J magnitude/specificity score (to maintain positive relationship, presented as 1/score) as calculated on 28-3ζ constructs (Figure 2F). Results in (C) represent means ± SEM of 4 separate donors (n = 4), and results in (D) and (E) represent results from 4 separate donors (n = 4) and 3 independent CAR-J assays (n = 3). Asterisk in (C) represents significant difference ($p < 0.05$) between the indicated group and all other groups, calculated using one-way ANOVA.

While all functional CAR-T cells retained their proliferative and effector capacities in the second challenge (F263 indicated slightly delayed expansion), only F265 and F269 CAR-T cells retained capacity for proliferation and strong tumor control during the third challenge (Figure 5).

Tonically Active CARs Can Have a Therapeutic Effect *In Vivo*

Finally, to compare the therapeutic potential of autoactivating and non-autoactivating CARs, F263, F265, and F269 CAR-T cells were tested for their anti-tumor function in immunodeficient mice with U87-vIII xenografts (Figure 6). NOD-scid-IL2γR2$^{-/-}$ (NSG) mice were implanted subcutaneously with U87-vIII cells followed by intra-tumoral delivery of T cells with 20%–25% CAR transduction. Here, F263, F265, and F269 CAR-T cells all dramatically slowed tumor growth (Figures 6A and 6C), with significantly reduced ($p < 0.05$) tumor size at day 24 (Figure 6B). Median survival was also increased ($p < 0.05$) by 50% in mice receiving CAR-T cells compared to control mice, while there were no differences between CAR-T cell groups (Figure 6C).

Interestingly, the autoactivating F263 CAR-T cells performed similarly (if not better) at controlling tumor growth compared to F265 or F269 (Figure 6). We hypothesize that this might be driven by the enhanced effector differentiation and, thus, the more immediate cytolytic killing of F263 observed in our *in vitro* co-culture experiments, thereby potentially making such tonically active CAR-T cells a desirable trait for use in treating aggressive tumor models such as that used here.

DISCUSSION

Although CAR-T cell therapy promises to revolutionize cancer treatment and introduce genetically engineered cell therapies as bona fide medicines, the current experience in solid tumor clinical trials would indicate that improvements to current CAR technology will be required to make this a reality outside of the realm hematological cancers. Fortunately, numerous aspects of CAR-T cells are amenable to process development and bioengineering modifications to upgrade its function. This includes T cell expansion conditions, using specific cellular sub-types, genome editing, and CAR construct

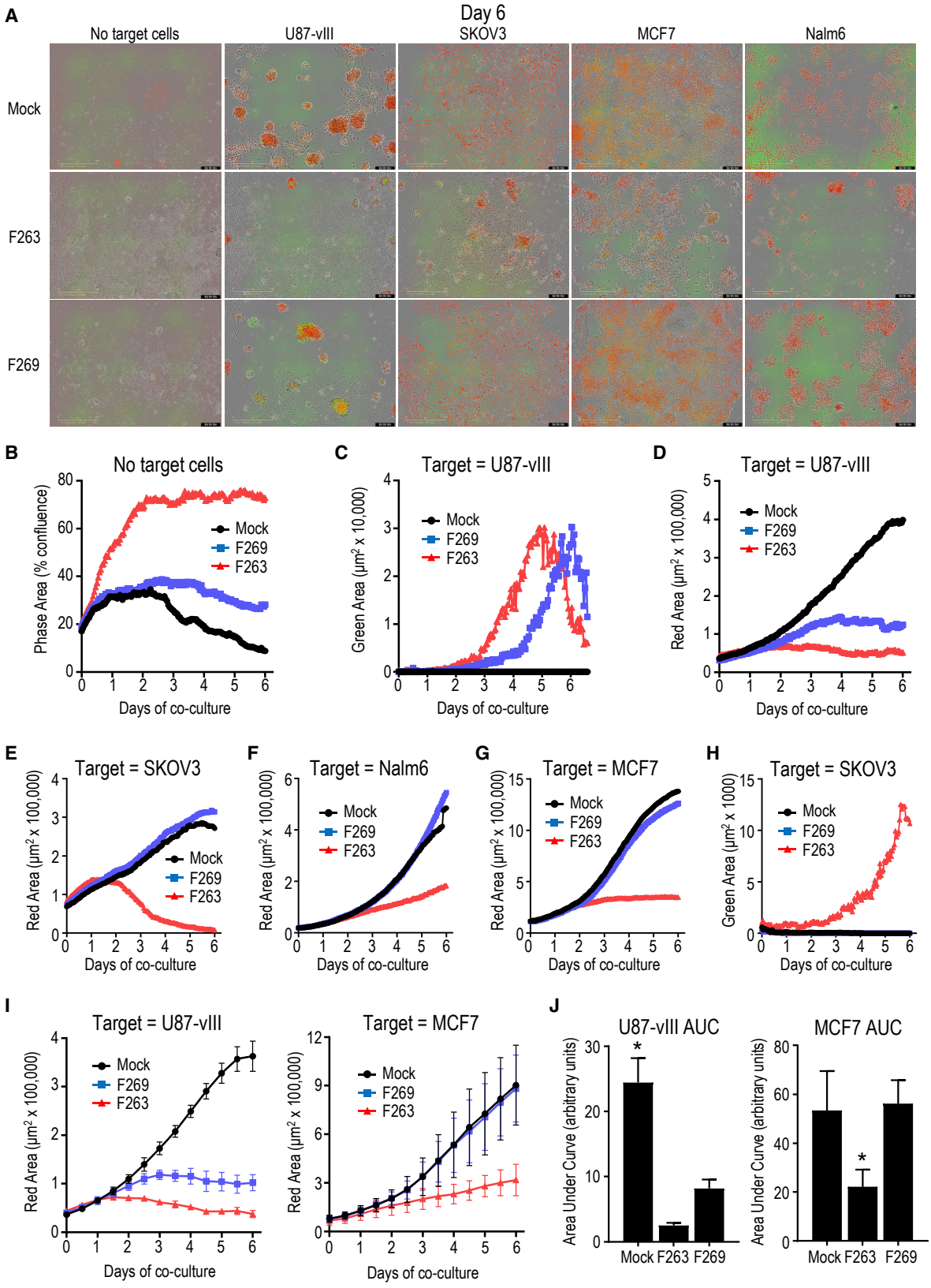

(legend on next page)

composition in addition to innumerable dosing and combination therapy strategies. Focusing on the construct itself offers a virtually limitless amount of engineering alterations to examine. Therefore, more and better screening tools for characterizing CARs are warranted and have great potential to improve CAR functionality.

Current designs for CAR ABDs rely heavily on antibody-binding characteristics. Although determining the immunochemical attributes of antibodies is a routine step in antibody development, we do not know whether or which antibody characteristics predict or correspond to their suitability as CARs.[20] While correlating antibody binding to CAR functionality allows ABDs to be short-listed (and for the generation of design guidelines), this strategy is still highly dependent on empirical validation in the context of a CAR-T cell assay. Instead of examining the interaction between a soluble antibody and a soluble antigen or antigen-expressing cell, the protocol described here assesses ABD binding in the most CAR-relevant way possible: as an antigen receptor expressed by a T cell. In fact, detecting surface CD69 expression induced by CAR expression in cellular co-cultures provides a functional readout that recapitulates better the context of CAR than purified antibody assays; incorporating gene translation, protein folding, surface expression, receptor interactions/clustering, epitope availability on target cells, target cell binding, stimulatory signaling, and transcriptional activation. Thereby, we propose that CAR-J provides more relevant information and quality control checks than antibody affinity measurements[9] and could potentially replace some antibody characteristic testing in the context of developing CARs.

Although CAR-J allows the generation of large datasets regarding tonic and antigen-specific CAR activity, the physiological insight of these observations remains unclear. Despite detecting the absence or presence and the magnitude of CAR-induced activation, this assay distills this response into a single parameter: surface CD69 expression. While GFP and APC were deliberately chosen to allow this protocol to be performed on standard 2-laser flow cytometers, T cells translate stimuli from the T cell receptor (TCR) itself, CD4/CD8, CD28, and various cytokine receptors to networks that ultimately converge on transcription factors such as NFAT, nuclear factor κB (NF-κB), and c-Jun/AP-1 to mediate cellular changes associated with T cell activation. Therefore, while surface CD69 is a reliable and canonical early marker of T cell activation, it may not reflect the nuances in antigen signaling induced by CARs. To supplement this, other activation markers (i.e., CD25)[21] could be measured; also, a Jurkat line has been created with response elements for NFAT, NF-κB, and c-Jun/AP-1 driving expression of different fluorescent proteins.[22–24] The correlation of Jurkat cell activation of these markers with the processes of T cell activation within primary T cells remains unclear, and based on the data provided here, we are skeptical of whether a Jurkat-based assay can ever fully predict the effects of a particular CAR molecule within primary T cells.

Assessing CAR activation in Jurkat cells may not adequately predict the impact that CAR molecules have on T cell differentiation, as the response to antigens manifests in cellular phenotypes ranging between T_{EFF} and T_{SCM}. For instance, CAR-T cells with 41BB co-stimulatory domains have shown better persistence, less exhaustion, improved tumor control, and preferred conversion to T_{CM} compared to those with CD28,[25–28] and recent work aims to tailor CAR signaling components to increase T cell persistence.[29] These diverse signaling-mediated responses likely cannot be examined in Jurkat cells and, instead, require testing in primary human T cells with stable CAR expression. Despite these drawbacks, we did observe here a strong correlation between CAR-J and human CAR-T cell function, particularly with respect to tonic signaling of CARs, whereby our novel EGFRvIII-targeting scFvs that produced relatively higher tonic/non-specific CAR-J activation also caused prolonged activation kinetics and non-specific killing when expressed in primary human CAR-T cells. Based on the data presented here, we believe a high-throughput CAR assay performed in Jurkat cells represents a viable first-pass procedure for the selection and optimization of novel CAR molecules.

Notably, the drop in gene synthesis costs combined with the robustness of next-generation gene assembly strategies (such as the restriction/ligation strategy used here) allows this protocol to be adapted to genuine high-throughput and potentially fully automated analyses. As the number of antigen targets and rational CAR designs continues to expand, the use of high-throughput screening assays for CAR development could represent a major tipping point allowing for the simultaneous assessment of thousands of constructs. In fact, we have begun using a strategy of CAR maturation where random mutationally or computationally designed libraries of ABD sequences are lentivirally delivered to Jurkat cells and subjected to rounds of response assessment and single-cell cloning to

Figure 4. CAR-J Predicts Human CAR-T Cell Function

Anti-EGFRvIII CAR-T cell effector function was assessed using continuous live-cell imaging of co-cultures between human CAR-T cells (GFP, green) and various cancer cell lines (stably expressing mKate2, red). (A) Representative images taken on day 6 from donor 2. (B) Autonomous T cell proliferation when cultured alone, as measured by assessing phase contrast. (C and D) Antigen-driven CAR-T cell proliferation, as measured by assessing GFP (C), and growth of target-specific cells, as measured by assessing mKate2 (D), during U87-vIII co-culture. (E–G) Growth of various EGFRvIII-negative cancer cell lines during co-culture with mock or EGFRvIII-CAR T cells. Targets were SKOV3 (E), Nalm6 (F), and MCF7 (G). (H) CAR-T cell proliferation during SKOV3 co-culture. (I) Average expansion of U87-vIII and MCF7 cells across 3 donors. (J) Area under the curve (AUC) measurements performed on data in (I). Scale bars represent 400 μm. Results shown in (B)–(H) are derived from donor 2 only but are representative of repeated experiments (see Figures S3–S5), while (I) and (J) represent donors 1, 2, and 4 ($n = 3$). Asterisks in (J) represent significant difference ($p < 0.05$) between the indicated group and all other groups, calculated using one-way repeated-measures ANOVA. Note that a technical issue was encountered during the experiment with donor 3, and *in vitro* killing assay was not possible.

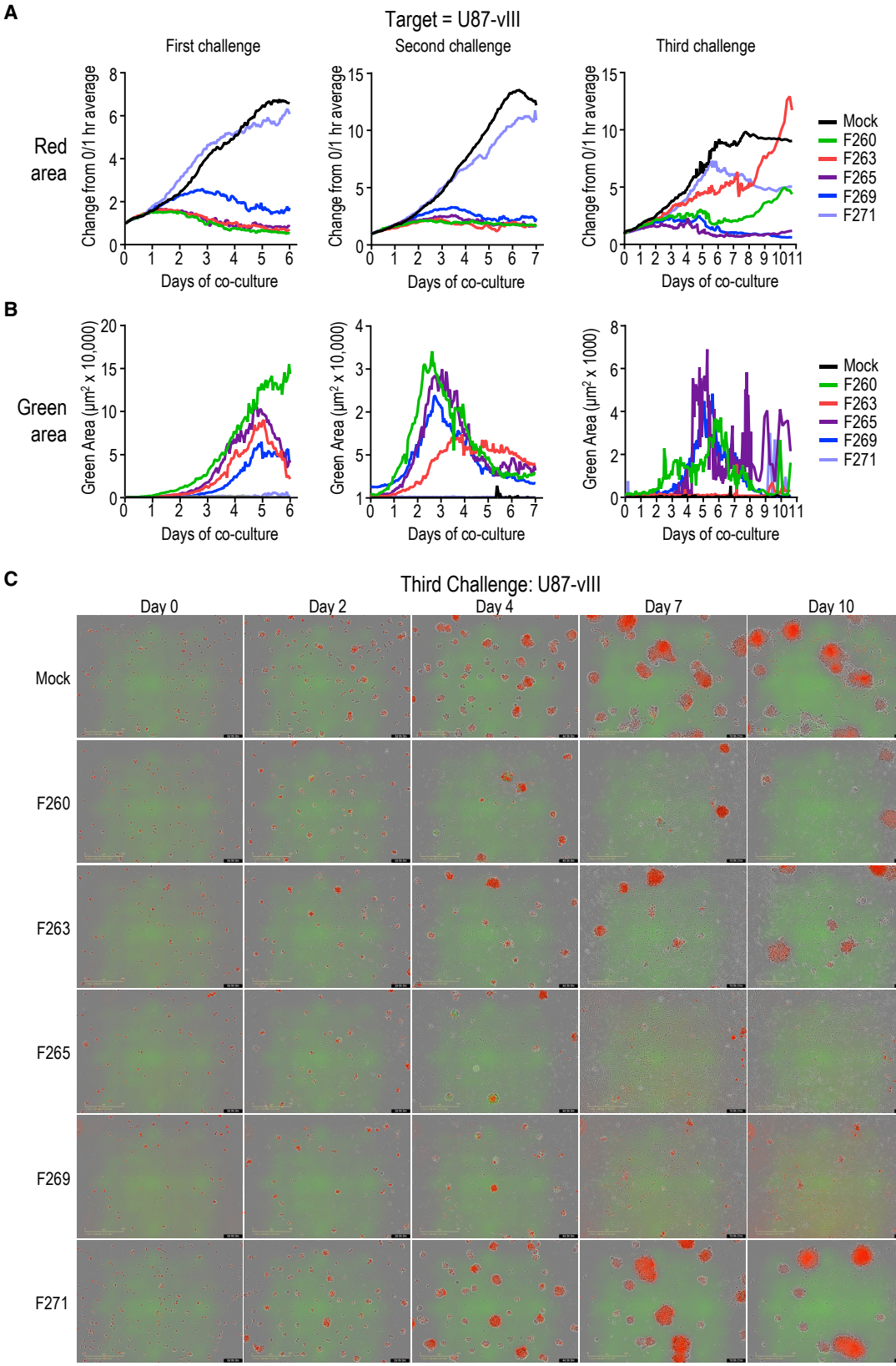

(legend on next page)

identify novel "hits" through CAR sequencing. Although deriving ABDs from antibodies is a tried-and-tested way of creating novel biological antigen-specific interacting domains, some or all of the processes of animal immunization, hybridoma generation, clonal screening, epitope maturation, and humanization can be theoretically bypassed by rational, library, and machine-learning strategies for CAR design, where functional activity, specificity, and cross-reactivity assessments are performed using CAR-J. Importantly, while we have largely presented a successful CAR design experiment here, we routinely encounter antigen-specific antibodies that do not cause target-specific Jurkat activation when incorporated into a CAR.

We have herein described a simple and high-throughput protocol that assesses CAR-mediated signaling specificity and magnitude in the context of an antigen receptor that is particularly well suited to screen scFvs for their on and off activation properties. Despite limitations regarding the physiological insight provided by Jurkat CD69 expression discussed earlier, we believe that the data presented here clearly demonstrate the value of this assay to determine a large amount of auto-activation, specificity, and sensitivity information regarding CAR function that can supplement and even replace some antibody characterization in order to short-list constructs for pre-clinical assessment. As CAR-T cell research intensifies and the therapeutic scope expands, straightforward methods to evaluate CARs and more quickly enable their optimization, and the *in vitro* assay described here, fill such a void.

MATERIALS AND METHODS

Cell Culture

Jurkat (ATCC), Raji (ATCC), Nalm6 (generously provided by Dr. Beat Bornhauser, University Children's Hospital Zurich), and DKMG (generously provided by Maria Jaramillo, National Research Council Canada) cells were cultured in standard RPMI media supplemented with 10% fetal bovine serum (FBS), 1% penicillin/streptomycin, 1 mM sodium pyruvate, 2 mM L-glutamine, and 55 μM mercaptoethanol at 37°C and 5% CO_2. MCF7 and SCOV3 cells (ATCC) were grown in similar DMEM-based media. The glioblastoma cell lines U87MG (U87, wild-type) and U87MG-vIII (U87-vIII, expressing EGFRvIII via retroviral transduction and sorting) were kindly provided by Professor Cavnee, from the Ludwig Institute for Cancer Research, University of California, San Diego (San Diego, CA, USA).[30,31] Cell lines were routinely confirmed to be mycoplasma-free using PCR.[32]

Primary human T cells were isolated from whole blood obtained from healthy human volunteers under informed consent and approval through the National Research Council of Canada Research Ethics Board. Briefly, peripheral blood mononuclear cells (PBMCs) were isolated from freshly obtained diluted whole blood (1:1 D-PBS) using density gradient centrifugation over Ficoll-Paque Plus (GE Healthcare) at 300 × *g* for 30 min. Pan T cells were purified from recuperated PBMCs by magnetic negative selection according to the manufacturer's instructions (Miltenyi Biotec), typically yielding >90% pure T cell fractions as assessed by flow cytometry. T cells were immediately activated with TransAct anti-CD3/CD28 matrix reagent according to the manufacturer's instructions (Miltenyi Biotec) and cultured in ImmunoCult XF expansion media (STEMCELL Technologies) supplemented with recombinant human IL-2 (rhIL2; 20 IU/mL; Proleukin, Novartis). Activated T cells were typically transduced with virus 24 h post-stimulation and then subsequently expanded in rhIL2-supplemented expansion media (20 IU/mL) with strict maintenance of cell concentrations below 500,000 cells/mL. All cell counting was performed using an automated cell counter (Cellometer; Nexcelcom) that assesses live/dead counts using acridine orange/propidium iodide (PI) staining.

Creating pSLCAR and pSLCAR-CD19

The simple lentiviral chimeric antigen receptor plasmid (pSLCAR) was derived from the Cas9/CRISPR lentiviral plasmid pLenti-CRISPR-EGFP (Addgene #75159). First, the U6 promoter and Cas9 sequences were removed from pLentiCRISPR-EGFP, and the RSV promoter was replaced with the CMV promoter/CAG enhancer from pHIV-EGFP (Addgene #21373). We subsequently inserted dual BsmBI/Esp3I restriction sites positioned in opposite directions between the EFS and the P2A sequence, creating an Esp3I restriction cassette (Figure 1C). Note that both LTR regions are truncated, thereby creating a self-inactivating 3′ LTR: this constitutes a 3rd-generation lentiviral plasmid capable of producing lentivirus after co-transfection into suitable cells (i.e., HEK293T) along with appropriate amounts of lentiviral envelope and polymerase protein plasmids such as pCMV-VSV-G (Addgene #8454) and psPAX2 (Addgene #12260).

We next inserted a CAR construct into the Esp3I restriction cassette containing a scFv from the often used mouse anti-human CD19 antibody FMC63,[10] thereby generating pSLCAR-CD19 (Figure 1C). We generated a plasmid construct similar to that developed by the National Cancer Institute (NCI),[33,34] which is available online.[10] The NCI's CAR construct contains: a signal peptide composed of the first 22 amino acids of the human GCSF2Rα subunit, a scFv composed of a heavy chain and a light chain derived from FMC63[34] connected by a unique linker peptide (GSTSGSGKPGSGEGSTKG),[35] the final 107 amino acids of human CD28 (39 from the topological domain, 27 from the transmembrane

Figure 5. Repeated Co-culture Re-challenge Leads to Loss of Effector Function for Auto-activating CARs

After 7 days of co-culture with U87-vIII cells (first challenge), EGFRvIII CAR-T cells generated from donor 4 were isolated, diluted, and used to conduct a similar co-culture assay with U87-vIII cells (second challenge). CAR-T cells cultured alongside U87-vIII cells for 7 days in the second challenge were then used to conduct a similar tertiary re-challenge assay (third challenge). (A) U87-vIII cell growth was assessed by measuring the change in mKate2 (red) area from the first two time points (0 and 1 h). (B) CAR-T cell expansion was assessed by the total GFP (green) area. (C) Representative images from the tertiary re-challenge experiment. Scale bars represent 400 μm.

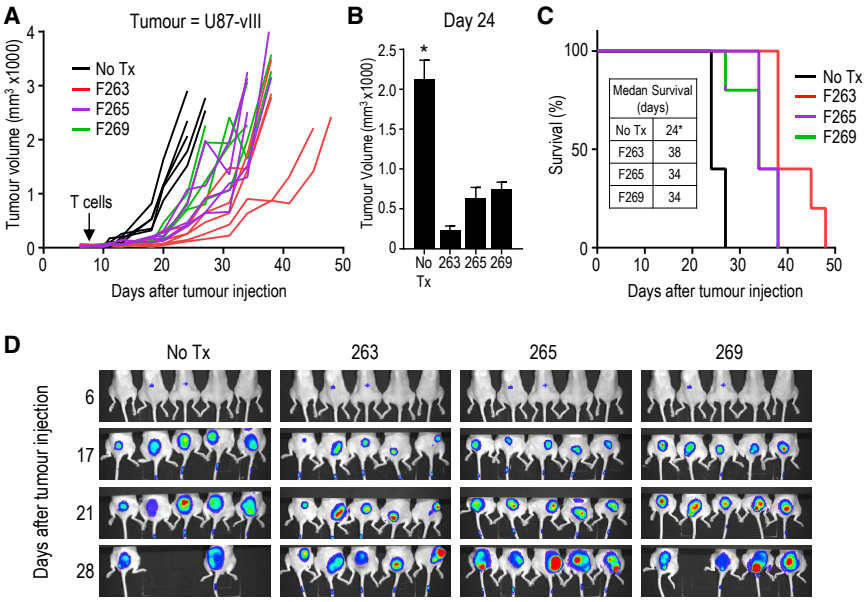

Figure 6. Anti-EGFRvIII CAR-T Cells Demonstrate Therapeutic Efficacy *In Vivo*

NSG mice were subcutaneously xenografted with U87-vIII tumor cells. One week later, the indicated CAR-T cells were prepared and injected intra-tumorally, after which tumor size and survival were measured. (A) Tumor growth as determined by thrice weekly caliper measurements. (B) Tumor size 24 days after tumor injection. (C) Kaplan-Meyer survival curve, with median survival numbers indicated. (D) Fluorescent *in vivo* imaging performed to visualize tumor growth of mKate-expressing U87-vIII cells. Asterisks in (B) and (C) represent significant difference ($p < 0.05$) between the indicated group and all other groups, calculated using one-way ANOVAs. Median survival was calculated using GraphPad Prism. n = 5 mice per group.

domain, and 41 from the intracellular domain), and 112 amino acids from human CD3ζ transcript variant 2 (which is missing a glutamine at position 101 compared to variant 1).

We modified this NCI construct so that, under control of the EFS, pSLCAR-CD19 contains in-frame sequences for: the human CD28 signal peptide, 3 tandem FLAG repeats, the anti-CD19 scFv from FMC63 (human codon optimized), the human CD8α hinge region (optimized to avoid secondary structures), the human CD28 transmembrane domain, the human CD28 cytoplasmic domain (optimized to avoid secondary structures), the human CD247/CD3ζ cytoplasmic domain, a P2A ribosomal skipping self-cleaving peptide, EGFP, and a single stop codon. Importantly, BpiI restriction sites exist between the CD28 signal peptide and the scFv, as well as between the CD8 hinge and CD28 transmembrane domains, creating a BpiI restriction cassette similar to the Esp3I cassette in pSLCAR (Figure 1C). This allows CAR specificity to be swapped for that of other antigens without needing to synthesize accessory CAR components. Additional restriction sites are located immediately before the CD8, CD3, and P2A sequences to easily allow exchanging of CAR signaling components.

To create pSLCAR-CD19 with other signaling domains, gene fragments (Twist Biosciences) were appropriately designed containing the desired sequences (41BB-CD3ζ, CD28-41BB-CD3ζ, and CD3ζ) and Gibson-cloned (using in-house made reaction buffer) into pSLCAR-CD19-28-3ζ previously digested with NheI and KpnI. pSLCAR-CD19-28tm was created by digesting pSLCAR-CD19-3ζ with NheI followed by T4 ligation, leaving the CD28 transmembrane domain (Figure S1A). Successful clones were confirmed by sequencing. These plasmids have been made available at Addgene (#135991, #135992, and #135993): please see Addgene for complete sequence information and plasmid maps.

Swapping the Antigen-Binding Domain in pSLCAR-CD19

Complete Protocol

The design for gene fragments to replace the FMC63-derived anti-CD19 scFv in pSLCAR-CD19 is presented in Figure 1G and in the following text. Our replacement scFv sequences are typically between 800 and 1,000 bp long. When designing these for performing "golden-gate" simultaneous restriction/ligation recombinations, the 5′ and 3′ ends (BpiI restriction cloning sites) are structured in the following manner: 5′-ATGGGGACA**GAAGAC**CTAGGA...*scFv and hinge sequence*...CCTTGG**GTCTTC**GGTA-3′, where bold indicates the BpiI restriction sites, the underlined GGA encodes the final in-frame amino acid (glycine) of the CD28 signal peptide, and the underlined CCT encodes the first in-frame residue (proline) of the subsequent CD28 transmembrane domain. To swap the CD19 scFv for one encoding an scFv against HER2, a recombination reaction was set up containing: 250 ng pSLCAR-CD19, 50 ng HER2 scFv DNA fragment (Twist Biosciences; roughly a 1:2 molar ratio), 0.25 μL BpiI (Thermo Fisher Scientific, ER1012), 0.25 μL T4 ligase (Thermo Fisher Scientific, 15224025), 4 μL T4 reaction buffer (Thermo Fisher Scientific), and topped up to 20 μL with molecular grade H_2O.[18] This reaction was then incubated as follows: (37°C for 10 min, 16°C for 10 min) × 5 cycles, 37°C for 60 min, 80°C for 5 min, and 4°C indefinitely. 5 μL of this reaction was used to transform DH5α chemically competent cells, which were plated on ampicillin-containing agar plates.

Gene fragments for replacing the anti-CD19 scFv can also be designed as compatible with Gibson assembly. It is recommended to design gene fragments with at least 40-bp overhangs on either side of the restriction sites to ensure high-efficiency insertion: our typical design is shown here: 5′-TGCTCTTGGCTCTCAACTTATTCCCTTCAATTCAAGTAACAGGA...*scFv and hinge sequence*...CCTTCTAAGCCCTTTTGGGTGCTGGTGGTGGTTGGTGGAGTCCT-3′, where the underlined GGA encodes a glycine residue in frame with the upstream Kozak and CD28 signal peptide sequences and the underlined CCT encodes a proline residue in frame with the subsequent CD28 transmembrane domain. After digesting pSLCAR-CD19 with BpiI,

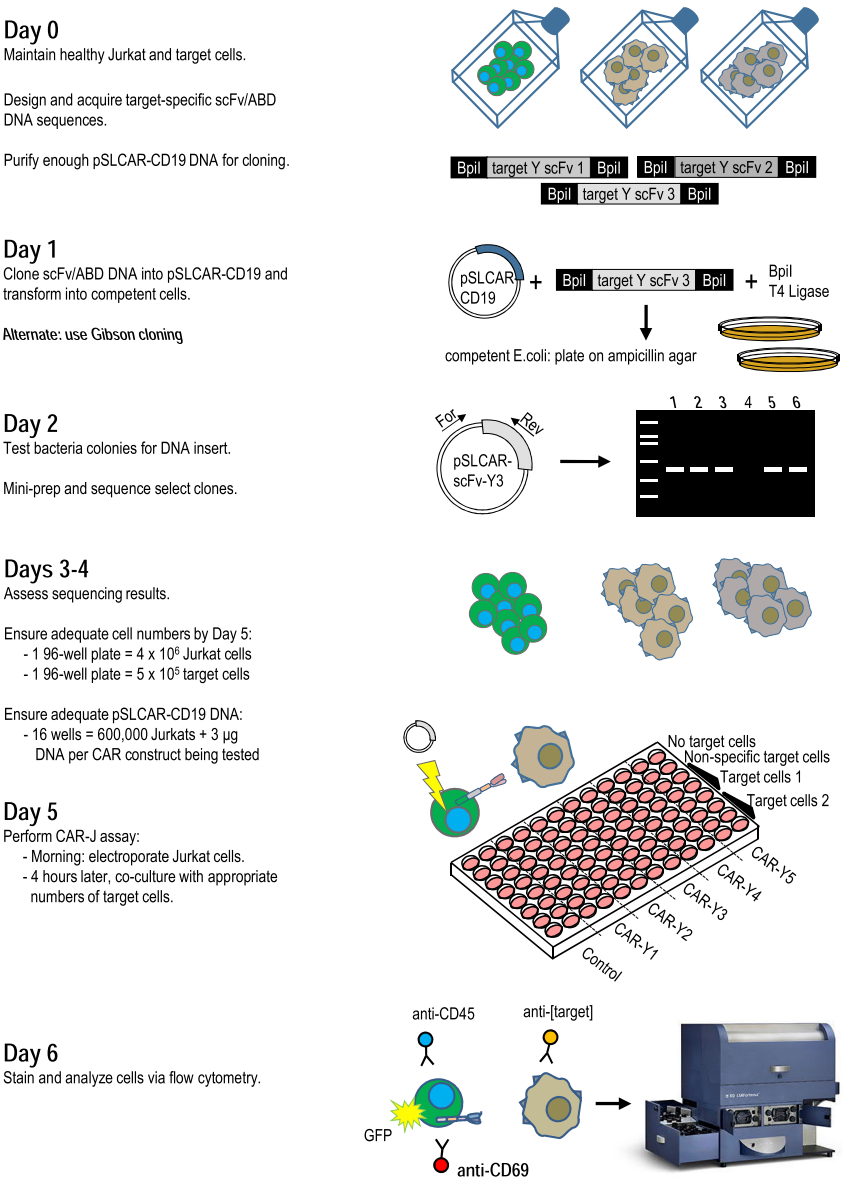

Figure 7. Overview of Complete CAR-J Screening Protocol

See Materials and Methods for a complete description of this protocol. See Figure S6 for a similar cartoon flow diagram outlining the rapid CAR-J protocol.

the 8,000-bp band was isolated and used in a Gibson assembly reaction along with the properly designed scFv gene fragment, and this reaction was transformed into chemically competent DH5α.

To confirm successful cloning, individual transformants were analyzed with PCR using CAR/scFv-specific primers. Colonies with predicted PCR products were then grown overnight in normal lysogeny broth (LB) and plasmid DNA was purified using standard mini-plasmid (Thermo Fisher Scientific) or midi-plasmid (QIAGEN) purification kits. Although both the restriction/ligation and Gibson assembly methods typically yield >99% success rates, it is recommended that 2–3 plasmids from successful colonies be sequenced to confirm construction.

Rapid Protocol

Due to the efficiency of Gibson assembly or the single-tube restriction/ligation strategy described here, this protocol was adapted to enable even higher throughput CAR screening (Figure S6). Mainly, this was achieved by skipping the PCR screening and sequencing aspects of inserting new scFv sequences into pSCLAR-CD19. Instead of plating the Gibson or restriction/ligation recombination reaction on ampicillin-containing agar plates, the reaction was transferred straight to ampicillin-containing LB. After overnight growth, this polyclonal plasmid population was purified and immediately used for performing functional CAR analyses.

Anti-EGFRvIII mAb Generation and Screening

All animal experiments were carried out in strict accordance with the National Research Council of Canada Animal Care policy and guidelines. Six-week old female A/J mice (The Jackson Laboratory, Bar Harbor, ME, USA) were injected intraperitoneally and subcutaneously with 100 µg EGFRvIII recombinant protein emulsified in Titermax adjuvant (Cedarlane Labs, Burlington, ON, Canada) at day 0 and in PBS without adjuvant at day 22. After 2–6 months, intraperitoneal and subcutaneous injections were re-administered 3 or 4 days prior to fusion experiment. Spleen cells were electrofused to the NS0 myeloma cell line using as described previously.[36,37] Hybridoma supernatants were screened for appropriate antigen specificity by ELISA on EGFRvIII and EGFR recombinant proteins. Briefly, half-area 96-well plates (Costar #3690) were coated with 25 µL per well of immunogen at 5 µg/mL in PBS and incubated overnight at 4°C. Microplates were washed three times in PBS and blocked for 30 min with PBS containing 1% bovine serum albumin (BSA; Sigma, catalog #A7030). Blocking buffer was removed, and 25 µL hybridoma supernatant was added. After 2-h incubation, microplates were washed 4 times with PBS-Tween 20 (0.05%) and 25 µL of a 1/5,000 dilution of alkaline-phosphatase-conjugated $F(ab')_2$ goat anti-mouse immunoglobulin G (IgG) (Fc specific, #115-056-071, Jackson Immunoresearch, Cedarlane, Burlington, ON, Canada) in blocking buffer was added. After 1-h incubation, microplates were washed 4 times, and

25 μL p-nitrophenyl phosphate (pNPP) substrate (Sigma-Aldrich Canada, Oakville, ON, Canada) at 1 mg/mL in carbonate buffer (pH 9.6) was added and further incubated for 1 h at 37°C. Absorbance was read at 405 nm using a SpectraMax 340 PC plate reader (Molecular Devices, Sunnyvale, CA, USA).

ELISA-positive antibodies were further characterized by flow cytometry on U87 and/or U87-vIII cells. Cells were harvested, centrifuged, and resuspended in complete medium at 2×10^6 cells/mL. 50 μL cells per well were distributed in a polypropylene V-bottom 96-well plate, and equal volumes of hybridoma supernatant were added and incubated for 2 h. Cells were washed twice by centrifugation and further incubated with a fluorescein isothiocyanate (FITC)-labeled $F(ab')_2$ goat anti-mouse antibody (Fc specific, #115-096-071, Jackson ImmunoResearch Laboratories, Cedarlane, Burlington, ON, Canada) for 1 h. Cells were washed and resuspended in medium containing PI to exclude dead cells from analysis. Samples were filtered through a 60-μm nylon mesh filter plate (Millipore, Cork, Ireland) to remove cell aggregates, and flow cytometry analyses were performed on PI-negative cells.

Anti-CD22 mAb Generation and Screening

Animals were immunized as described earlier using CD22 recombinant antigen. Hybridoma supernatants were screened for appropriate specificity by ELISA on CD22 and a panel of eight unrelated antigens. ELISA-positive antibodies were further characterized by flow cytometry on Ramos (CD22+), U266 (CD22−), or Jurkat (CD22−) cell lines as described earlier.

Hybridoma Sequencing

Select hybridomas were recloned to ensure monoclonality and sequenced. Briefly, mRNA was extracted from hybridoma cell pellet (Dynabeads mRNA DIRECT Purification Kit, Thermo Fisher Scientific) and reverse transcribed into cDNA (Maxima H Minus First Strand cDNA Synthesis Kit, Thermo Fisher Scientific, Waltham, MA, USA). Samples of DNA encoding VH and VL domains were PCR amplified (Platinum 2X Hot Start Master Mix, Invitrogen; or Q5 HotStart High Fidelity 2X Master Mix, New England Biolabs) using either mixtures of degenerate forward primers annealing in FR1 or a custom 5′ primer sequence introduced in cDNA synthesis using a template-switching oligo in combination with a single reverse primer annealing in CH1 (Mouse Ig-Primer Set, Novagen). The resulting amplicons were sequenced using an ABI 3730XL sequencer. Alternatively, a sequencing library was constructed with the resulting indexed amplicons (TrueSeq LT Indexes, Illumina) and sequenced on a MiSeq System (MiSeq Reagent Nano Kit, v.2 [500 cycles], Illumina).

Jurkat Transfection

Jurkat cells were transfected via electroporation according to a previously outlined protocol.[38] After collection via centrifugation at $300 \times g$, 5×10^5 to 5×10^6 cells were suspended in 100 μL Buffer 1SM (5 mM KCl, 15 mM $MgCl_2$, 120 mM Na_2HPO_4/NaH_2PO_4, 25 mM sodium succinate, and 25 mM mannitol [pH 7.2]) and briefly (<5 min) incubated with appropriate plasmid DNA (2–5 μg). This solution was transferred into 0.2-cm generic electroporation cuvettes (Bio-Rad Gene Pulser) and immediately electroporated using a Lonza Nucleofector I and X-01 program (X-001 on newer Nucleofector models). Cells were then cultured in pre-warmed recovery media consisting of RPMI with 20% FBS, 2 mM L-glutamine, and 1 mM sodium pyruvate. Cell:DNA ratios for optimal gene expression should be empirically determined.

CAR-J Activation

Jurkat activation was assessed using flow cytometry detection of GFP (FITC) and surface CD69 expression using an APC-conjugated anti-human CD69 antibody (Becton Dickinson, BD #555533). Cells were not washed prior to or after staining: 0.2 μL antibody was added to 50 μL PBS per well of the 96-well plate; this diluted antibody solution was added to wells, cells were incubated for 30 min at 37°C, formaldehyde was added to a final concentration of 0.5%, and the plate was immediately analyzed. In the proof-of-concept experiment in Figures 1D–1F, cells were additionally stained with 0.1 μL anti-CD45 BV786 (BD Biosciences, #563716) per well to demonstrate a potential gating strategy. Such additional markers may be included and required in application-dependent situations (i.e., GFP-expressing stable knockdown or knockin target cell lines). All flow cytometry analyses were performed using a BD LSRFortessa configured with a high-throughput plate reader and the following lasers: 355 nm, 405 nm, 488 nm, 561 nm, and 640 nm. CD69 expression was determined by the mean fluorescence intensity (MFI) of the compensated APC channel (excitation [ex.], 640; emission [em.], 670/14).

Human T Cell Phenotyping

A multi-color flow cytometry panel was designed to assess T cell phenotype markers. At select time points during expansion, T cells were stained using an antibody cocktail (CD4-BUV395, CD8-APC-H7, CD25-PE-Cy7, CD27-BUV737, CD45RA-BV650, CD45RO-PE-CF594, CD69-BV786, CD197/CCR7-PE, and CD279/PD1-BV421; BD Biosciences) diluted in staining solution (1:1 mixture of Brilliant Stain Buffer Plus [BD Biosciences, #566385] and PBS with 1% FBS, 10 mM HEPES, and 2 mM EDTA) for 30 min at room temperature, centrifuged, re-suspended in fixation solution (1% formaldehyde in PBS), and immediately analyzed.

Lentivirus Production

EGFRvIII-CAR lentiviral particles were generated using a HEK-based inducible packaging cell line grown in suspension in serum-free media, as previously described.[39] Briefly, cells were transfected at 1×10^6 cells/mL with 0.5 μg/mL transfer plasmid and PEIpro (Polyplus) at a ratio of 2, and sodium butyrate was added 18 h later to induce virus production. Supernatants containing virus particles were collected approximately 72 h post-transfection and centrifuged at $3{,}000 \times g$ for 15 min at 4°C to remove cell debris. At the time of harvesting, the viral supernatant was filtered through a 0.45-μm polyvinylidene fluoride (PVDF) filter (Millipore), underlaid with a 20% (w/v) sucrose cushion, and concentrated by ultracentrifugation using

an Optima L-80 XP (Beckman Coulter) for 3 h at 37,000 × *g* at 4°C. The supernatant was carefully discarded, and the pelletable fraction was suspended in RPMI plus 10% FBS. Lentiviral particle concentration was determined by transducing HEK293A cells with serial dilutions. Cells were analyzed for GFP expression using flow cytometry 3 days post-transduction.

Human T Cell Transduction

T cells were transduced with CAR lentivirus via spinoculation. 24 h after adding T cell activation reagent, cells were washed and isolated for transduction: for each CAR, 500,000 cells were given lentivirus, MOI = 10, in a final volume of 1 mL XF Expansion Media and centrifuged at 2,000 rpm for 2 h at 30°C. After centrifugation, cells were placed in a cell culture incubator for 2 h before being re-suspended in 5 mL XF Expansion Media with 20 U/mL rhIL2 (100,000 cells/mL). The next day, cells were given fresh IL-2-containing media and expanded as previously outlined.

Human CAR-T Cell Proliferation and Cytotoxicity

Continuous live-cell imaging (IncuCyte S3, Sartorius) was used to assess CAR-T cell expansion and cytotoxicity. To more easily visualize target cells, stable lines (Nalm6, SKOV3, MCF7, and U87-vIII) expressing nuclear-localized mKate2 were generated using commercially obtained lentivirus (Lenti Nuclight-Red, Incucyte, Sartorius). Using cells 9 days after CAR transduction, T cells were co-cultured with mKate2-labeled cancer cells at specific ratios in XF Expansion Media containing 20 U/mL rhIL2 and imaged every 30–60 min in light/phase as well as green (ex., 440–480 nm; em., 504–544 nm) and red (ex., 565–605 nm; em., 625–705 nm) fluorescent channels for up to 9 days. After proper image calibration, this software package allows phase, green, and red object counts and area assessments, enabling determination of GFP-positive CAR-T cell and mKate2-positive target cell confluence in the visual field.

Mice and *In Vivo* Experiment

NSG mice acquired from the Jackson Laboratory (JAX #005557) were used to assess therapeutic CAR-T cell function using human cell xenografts. Animals were housed according to proper institutional and Canadian Council on Animal Care guidelines. At an average age of 40 weeks, mice were subcutaneously injected with 1×10^6 fluorescently labeled U87-vIII cells described earlier, a number that we previously determined to consistently produce a palpable tumor within 7 days. Eight days after tumor cell injection, cryopreserved CAR-T cells were thawed and washed with PBS, and 1×10^7 total T cells (with 20%–25% CAR transduction) were immediately delivered intra-tumorally, ensuring equal distribution of tumor sizes between groups. Tumor growth was evaluated three times per week using calipers by trained animal technicians blinded to specific treatment groups. The primary endpoint was tumor size above 2,000 mm^3, with secondary endpoints determined by overall animal health and well-being. Mice were also assessed for tumor growth using IVIS *in vivo* imaging to examine red fluorescence derived from the NLS-mKate2-marked U87-vIII cells.

CAR Magnitude/Specificity Score

We determined a metric to more easily compare CAR responses in large datasets. This score is simply the ratio of specific activation to non-specific activation, or CAR-J CD69-APC-MFI in response to cells expressing the target antigen compared to CD69-APC-MFI in response to cells not expressing the target antigen. It was calculated in the following manner.

$$(\text{CD69} - \text{APC} - \text{MFI caused by target} - \text{specific cell type}) \div (\text{average CD69} - \text{APC} - \text{MFIcaused by non} - \text{specific cell types})$$

$$\text{For EGFRvIII CARs} = (\text{APC caused by U87} - \text{vIII}) \div (((\text{APC caused by Nalm6}) + (\text{APC caused by MCF7})) \div 2)$$

$$\text{For CD19 CAR} = (\text{APC caused by Nalm6}) \div (((\text{APC caused by U87} - \text{vIII}) + (\text{APC caused by MCF7})) \div 2)$$

Therefore, this score will be affected by the strength of target-specific activation as well as how specific the CAR is for the target antigen.

Statistics

Quantified results presented are means ± standard error of the mean (SEM) and typically represent 3 independently run experiments; specific experiment descriptions are contained in the respective figure legends.

Statistical comparisons were performed in appropriate situations where group size and replication numbers were not predetermined for power effects. t tests were calculated using Microsoft Excel and ANOVA analyses were performed using GraphPad Prism. Tukey's multiple comparison post hoc was used to identify locations of significance for ANOVAs. A p value of 0.05 was considered statistically significant in all situations. Analysis specifics and descriptions are included in the corresponding figure legends.

GraphPad Prism's linear regression function was used to perform the correlation analysis between CAR-J CD69 and human CAR-T cell CD25 in Figure 3. Median survival (Figure 6) was determined using GraphPad's survival analysis function.

Description of Complete High-Throughput CAR-J Assay

General guidelines for conducting a CAR-J screening assay are outlined later (Figure 6; Figure S6). Here, we describe an experiment similar to the one depicted in Figure 2A: testing 5 experimental CARs and one control CAR against 2 target cell lines performed in a single 96-well plate. However, this setup can be altered to conduct any assay of interest. Using a single 96-well plate, it is possible to: (1) screen 6 constructs against 2 target cell lines at titered ratios and 1 antigen-negative cell line (described here), (2) screen 6 constructs against a single cell line at 8 effector:target ratios, (3) screen 6 constructs at an individual ratio against 7 different cell lines, (4) compare a single construct to a control against 23 cell lines at a single ratio, or (5) screen 12 constructs against 3 cell lines at a single ratio.

Cells

Maintain healthy Jurkat and target cells by following standard culturing guidelines (ATCC). Most cancer cell lines, including Jurkat, should be split 2–3 times per week or before becoming confluent (2×10^6/mL for most suspension cells). By the day the assay is performed, 4×10^6 viable Jurkat cells and 5×10^5 of each target cell will be required for each 96-well plate.

Plasmids

Appropriately design new/donor scFv sequences *in silico* according to the format described herein for restriction/ligation or Gibson assembly, and synthesize these gene fragments. Insert these fragments into pSCLAR-CD19, and confirm plasmid construction with sequencing. Generate plasmid DNA using standard mini- or midi-prep purification procedures: by the day the assay is performed, 3 μg plasmid DNA will be required for each CAR construct being tested, including a control construct (typically, pSLCAR-CD19). Each mini-prep plasmid purification typically yields enough DNA for 8–10 assays performed in this manner.

Electroporation

Isolate Jurkat cells via centrifugation for 5 min at $300 \times g$, count, ensure viability >90%, and re-suspend them in 100-μL (Buffer 1SM) aliquots of 6×10^5 cells. Add 3 μg plasmid DNA and electroporate. Transfer this roughly 100 μL solution to 900 μL pre-warmed recovery media, giving a concentration of 6×10^5 cells/mL (30,000/50 μL). Allow cells to recover for 4 h.

Assay Setup

Remove and isolate each target cell line from culture, count, and re-suspend 5×10^5 cells in 833 μL R10 (6×10^5 cells/mL). Make a 1:10 dilution by transferring 100 μL into 900 μL R10 (final = 6×10^4 cells/mL), and make a second 1:10 dilution of the first diluted mixture by transferring 100 μL into 900 μL R10 (final = 6×10^3 cells). This way, 50 μL of the original cell mixture contains 30,000 cells, 50 μL of the first dilution contains 3,000 cells, and 50 μL of the second dilution contains 300 cells. Transfer 50 μL of each cell dilution into individual wells in a single row of a 96-well round-bottom and flow-cytometry-suitable plate, so that, for example, row C contains 50 μL of the second dilution of cell line 1 (300 cells per well), row D contains 50 μL of the first dilution of cell line 1 (3,000 cells per well), and row E contains 50 μL of the original mixture of cell line 1 (30,000 cells per well) (see Figures 2A and 6; Figure S6). Similarly fill rows F, G, and H with cell line 2. Fill row B with 50 μL containing 3×10^4 cells per well of an antigen-negative cell line of interest, and fill row A with 50 μL R10.

After allowing electroporated Jurkat cells to recover in antibiotic-free media for 4 h, transfer 50 μL of media/cells expressing individual CAR constructs into paired columns of the 96-well plate containing the target cell lines just described (see Figures 2A and 6; Figure S6). Incubate cells overnight. In this setup, columns 1 and 2 are technical replicates of Jurkat cells expressing CAR construct 1 (control anti-CD19), where row A contains CAR-J cells at an effector:target ratio of 1:0, row B contains CAR-J cells incubated with an antigen-negative cell line at an effector:target ratio of 1:1, row C contains CAR-J cells incubated with target cell line 1 at an effector:target ratio of 100:1, row D contains CAR-J cells incubated with target cell line 1 at an effector:target ratio of 10:1, and so forth.

Assay Detection

After overnight incubation (typically, 24 h after electroporation), dilute 22 μL APC-conjugated anti-human CD69 antibody in 5.5 mL PBS: this is enough for 110 wells at 0.2 μL antibody per well. Transfer 50 μL of this mixture into each well of the 96-well plate containing CAR-J and target cells. Allow cells to incubate at 37°C for 30 min, fix them in formaldehyde, and immediately analyze using flow cytometry.

This entire procedure would be performed 3 times using 3 separate Jurkat electroporation trials.

Data Availability Statement

The authors can confirm that all relevant data are included in this paper and/or the Supplemental Information files. Raw data can be provided upon request.

SUPPLEMENTAL INFORMATION

Supplemental Information can be found online at https://doi.org/10.1016/j.omtm.2020.01.012.

AUTHOR CONTRIBUTIONS

Study conception and design: D.B., S. McComb, and R.D.W. Manuscript writing: D.B., S. McComb, and R.D.W. Data analysis and interpretation and figure preparation: D.B. and S. McComb. Final manuscript and figure approval: all authors. Experimental procedures and data acquisition: D.B., T.N., S. MacLean, and A.Z. Anti-EGFRvIII mouse MAb development: J.A., J.L., D.H., A.F., and A.M. Human PBMC procurement and T cell isolation: R.A.P. Lentivirus production: C.G. and R.G.

CONFLICT OF INTERESTS

All authors of the manuscript are employees of the National Research Council Canada and received no outside assistance or influence regarding its content. D.B., A.M., S. McComb, and R.D.W. are co-inventors of a provisional patent application by the National Research Council Canada regarding novel EGFRvIII-based CAR-targeting domains (U.S. Provisional Application No. 62/824,391).

ACKNOWLEDGMENTS

The authors thank Annie Aubry for technical assistance, the anonymous PBMC donors, and the blood donation team at the Ottawa General Hospital. All work was supported by funds provided by the National Research Council Canada.

REFERENCES

1. Kochenderfer, J.N., Dudley, M.E., Kassim, S.H., Somerville, R.P.T., Carpenter, R.O., Stetler-Stevenson, M., Yang, J.C., Phan, G.Q., Hughes, M.S., Sherry, R.M., et al.

(2015). Chemotherapy-refractory diffuse large B-cell lymphoma and indolent B-cell malignancies can be effectively treated with autologous T cells expressing an anti-CD19 chimeric antigen receptor. J. Clin. Oncol. *33*, 540–549.

2. Park, J.H., Rivière, I., Gonen, M., Wang, X., Sénéchal, B., Curran, K.J., Sauter, C., Wang, Y., Santomasso, B., Mead, E., et al. (2018). Long-term follow-up of CD19 CAR therapy in acute lymphoblastic leukemia. N. Engl. J. Med. *378*, 449–459.

3. Maude, S.L., Laetsch, T.W., Buechner, J., Rives, S., Boyer, M., Bittencourt, H., Bader, P., Verneris, M.R., Stefanski, H.E., Myers, G.D., et al. (2018). Tisagenlecleucel in children and young adults with B-cell lymphoblastic leukemia. N. Engl. J. Med. *378*, 439–448.

4. Grigor, E.J.M., Fergusson, D.A., Haggar, F., Kekre, N., Atkins, H., Shorr, R., Holt, R.A., Hutton, B., Ramsay, T., Seftel, M., et al. (2017). Efficacy and safety of chimeric antigen receptor T-cell (CAR-T) therapy in patients with haematological and solid malignancies: protocol for a systematic review and meta-analysis. BMJ Open *7*, e019321.

5. Hartmann, J., Schüßler-Lenz, M., Bondanza, A., and Buchholz, C.J. (2017). Clinical development of CAR T cells-challenges and opportunities in translating innovative treatment concepts. EMBO Mol. Med. *9*, 1183–1197.

6. Townsend, M.H., Shrestha, G., Robison, R.A., and O'Neill, K.L. (2018). The expansion of targetable biomarkers for CAR T cell therapy. J. Exp. Clin. Cancer Res. *37*, 163.

7. Oldham, R.A.A., and Medin, J.A. (2017). Practical considerations for chimeric antigen receptor design and delivery. Expert Opin. Biol. Ther. *17*, 961–978.

8. Oren, R., Hod-Marco, M., Haus-Cohen, M., Thomas, S., Blat, D., Duvshani, N., Denkberg, G., Elbaz, Y., Benchetrit, F., Eshhar, Z., et al. (2014). Functional comparison of engineered T cells carrying a native TCR versus TCR-like antibody-based chimeric antigen receptors indicates affinity/avidity thresholds. J. Immunol. *193*, 5733–5743.

9. Bloemberg, D., McComb, S., and Weeratna, R. (2019). Building a better CAR: emerging high-throughput *in vitro* tools for CAR selection and optimization. Cell & Gene Therapy Insights *5*, 681–692.

10. (2012). Synthetic construct FMC63-28Z receptor protein gene, complete cds. https://www.ncbi.nlm.nih.gov/nuccore/HM852952.1.

11. Schneider, U., Schwenk, H.U., and Bornkamm, G. (1977). Characterization of EBV-genome negative "null" and "T" cell lines derived from children with acute lymphoblastic leukemia and leukemic transformed non-Hodgkin lymphoma. Int. J. Cancer *19*, 621–626.

12. Abraham, R.T., and Weiss, A. (2004). Jurkat T cells and development of the T-cell receptor signalling paradigm. Nat. Rev. Immunol. *4*, 301–308.

13. Duong, C.P.M., Westwood, J.A., Yong, C.S.M., Murphy, A., Devaud, C., John, L.B., Darcy, P.K., and Kershaw, M.H. (2013). Engineering T cell function using chimeric antigen receptors identified using a DNA library approach. PLoS ONE *8*, e63037.

14. Alvarez-Vallina, L., and Hawkins, R.E. (1996). Antigen-specific targeting of CD28-mediated T cell co-stimulation using chimeric single-chain antibody variable fragment-CD28 receptors. Eur. J. Immunol. *26*, 2304–2309.

15. Lipowska-Bhalla, G., Gilham, D.E., Hawkins, R.E., and Rothwell, D.G. (2013). Isolation of tumor antigen-specific single-chain variable fragments using a chimeric antigen receptor bicistronic retroviral vector in a mammalian screening protocol. Hum. Gene Ther. Methods *24*, 381–391.

16. Alonso-Camino, V., Sánchez-Martín, D., Compte, M., Nuñez-Prado, N., Diaz, R.M., Vile, R., and Alvarez-Vallina, L. (2013). CARbodies: human antibodies against cell surface tumor antigens selected from repertoires displayed on T cell chimeric antigen receptors. Mol. Ther. Nucleic Acids *2*, e93.

17. Cho, H.-S., Mason, K., Ramyar, K.X., Stanley, A.M., Gabelli, S.B., Denney, D.W., Jr., and Leahy, D.J. (2003). Structure of the extracellular region of HER2 alone and in complex with the Herceptin Fab. Nature *421*, 756–760.

18. Engler, C., Kandzia, R., and Marillonnet, S. (2008). A one pot, one step, precision cloning method with high throughput capability. PLoS ONE *3*, e3647.

19. Gan, H.K., Cvrljevic, A.N., and Johns, T.G. (2013). The epidermal growth factor receptor variant III (EGFRvIII): where wild things are altered. FEBS J. *280*, 5350–5370.

20. Gacerez, A.T., Arellano, B., and Sentman, C.L. (2016). How chimeric antigen receptor design affects adoptive T cell therapy. J. Cell. Physiol. *231*, 2590–2598.

21. Shatrova, A.N., Mityushova, E.V., Aksenov, N.A., and Marakhova, I.I. (2015). CD25 expression on the surface of Jurkat cells. Cell Tissue Biol. *9*, 364–370.

22. Jutz, S., Leitner, J., Schmetterer, K., Doel-Perez, I., Majdic, O., Grabmeier-Pfistershammer, K., Paster, W., Huppa, J.B., and Steinberger, P. (2016). Assessment of costimulation and coinhibition in a triple parameter T cell reporter line: Simultaneous measurement of NF-κB, NFAT and AP-1. J. Immunol. Methods *430*, 10–20.

23. Rosskopf, S., Leitner, J., Paster, W., Morton, L.T., Hagedoorn, R.S., Steinberger, P., and Heemskerk, M.H.M. (2018). A Jurkat 76 based triple parameter reporter system to evaluate TCR functions and adoptive T cell strategies. Oncotarget *9*, 17608–17619.

24. Rydzek, J., Nerreter, T., Peng, H., Jutz, S., Leitner, J., Steinberger, P., Einsele, H., Rader, C., and Hudecek, M. (2019). Chimeric antigen receptor library screening using a novel NF-κB/NFAT reporter cell platform. Mol. Ther. *27*, 287–299.

25. Carpenito, C., Milone, M.C., Hassan, R., Simonet, J.C., Lakhal, M., Suhoski, M.M., Varela-Rohena, A., Haines, K.M., Heitjan, D.F., Albelda, S.M., et al. (2009). Control of large, established tumor xenografts with genetically retargeted human T cells containing CD28 and CD137 domains. Proc. Natl. Acad. Sci. USA *106*, 3360–3365.

26. Long, A.H., Haso, W.M., Shern, J.F., Wanhainen, K.M., Murgai, M., Ingaramo, M., Smith, J.P., Walker, A.J., Kohler, M.E., Venkateshwara, V.R., et al. (2015). 4-1BB costimulation ameliorates T cell exhaustion induced by tonic signaling of chimeric antigen receptors. Nat. Med. *21*, 581–590.

27. Haso, W., Qin, H., Zhang, L., Orentas, R.J., and Fry, T.J. (2013). CD22-targeted chimeric antigen receptor (CAR) T cells containing the 4-1BB costimulatory domain demonstrate enhanced persistence and superior efficacy against B-cell precursor acute lymphoblastic leukemia (ALL) compared to those containing CD28. Blood *122*, 1431.

28. Kawalekar, O.U., O'Connor, R.S., Fraietta, J.A., Guo, L., McGettigan, S.E., Posey, A.D., Jr., Patel, P.R., Guedan, S., Scholler, J., Keith, B., et al. (2016). Distinct signaling of coreceptors regulates specific metabolism pathways and impacts memory development in CAR T cells. Immunity *44*, 380–390.

29. Kagoya, Y., Tanaka, S., Guo, T., Anczurowski, M., Wang, C.-H., Saso, K., Butler, M.O., Minden, M.D., and Hirano, N. (2018). A novel chimeric antigen receptor containing a JAK-STAT signaling domain mediates superior antitumor effects. Nat. Med. *24*, 352–359.

30. Abulrob, A., Giuseppin, S., Andrade, M.F., McDermid, A., Moreno, M., and Stanimirovic, D. (2004). Interactions of EGFR and caveolin-1 in human glioblastoma cells: evidence that tyrosine phosphorylation regulates EGFR association with caveolae. Oncogene *23*, 6967–6979.

31. Nishikawa, R., Ji, X.D., Harmon, R.C., Lazar, C.S., Gill, G.N., Cavenee, W.K., and Huang, H.J. (1994). A mutant epidermal growth factor receptor common in human glioma confers enhanced tumorigenicity. Proc. Natl. Acad. Sci. USA *91*, 7727–7731.

32. Molla Kazemiha, V., Shokrgozar, M.A., Arabestani, M.R., Shojaei Moghadam, M., Azari, S., Maleki, S., Amanzadeh, A., Jeddi Tehrani, M., and Shokri, F. (2009). PCR-based detection and eradication of mycoplasmal infections from various mammalian cell lines: a local experience. Cytotechnology *61*, 117–124.

33. Kochenderfer, J.N., Feldman, S.A., Zhao, Y., Xu, H., Black, M.A., Morgan, R.A., Wilson, W.H., and Rosenberg, S.A. (2009). Construction and preclinical evaluation of an anti-CD19 chimeric antigen receptor. J. Immunother. *32*, 689–702.

34. Kochenderfer, J.N., Wilson, W.H., Janik, J.E., Dudley, M.E., Stetler-Stevenson, M., Feldman, S.A., Maric, I., Raffeld, M., Nathan, D.A., Lanier, B.J., et al. (2010). Eradication of B-lineage cells and regression of lymphoma in a patient treated with autologous T cells genetically engineered to recognize CD19. Blood *116*, 4099–4102.

35. Cooper, L.J.N., Topp, M.S., Serrano, L.M., Gonzalez, S., Chang, W.-C., Naranjo, A., Wright, C., Popplewell, L., Raubitschek, A., Forman, S.J., and Jensen, M.C. (2003). T-cell clones can be rendered specific for CD19: toward the selective augmentation of the graft-versus-B-lineage leukemia effect. Blood *101*, 1637–1644.

36. Manceur, A.P., Zou, W., Marcil, A., Paquet, E., Gadoury, C., Jaentschke, B., Li, X., Petiot, E., Durocher, Y., Baardsnes, J., et al. (2017). Generation of monoclonal pan-hemagglutinin antibodies for the quantification of multiple strains of influenza. PLoS ONE *12*, e0180314.

37. Sun, Y., Gadoury, C., Hirakawa, M.P., Bennett, R.J., Harcus, D., Marcil, A., and Whiteway, M. (2016). Deletion of a Yci1 domain protein of *Candida albicans* allows homothallic mating in *MTL* heterozygous cells. MBio *7*, e00465–e16.

38. Chicaybam, L., Sodre, A.L., Curzio, B.A., and Bonamino, M.H. (2013). An efficient low cost method for gene transfer to T lymphocytes. PLoS ONE *8*, e60298.

39. Broussau, S., Jabbour, N., Lachapelle, G., Durocher, Y., Tom, R., Transfiguracion, J., Gilbert, R., and Massie, B. (2008). Inducible packaging cells for large-scale production of lentiviral vectors in serum-free suspension culture. Mol. Ther. *16*, 500–507.

OMTM, Volume *16*

Supplemental Information

A High-Throughput Method for Characterizing Novel Chimeric Antigen Receptors in Jurkat Cells

Darin Bloemberg, Tina Nguyen, Susanne MacLean, Ahmed Zafer, Christine Gadoury, Komal Gurnani, Anindita Chattopadhyay, Josée Ash, Julie Lippens, Doreen Harcus, Martine Pagé, Annie Fortin, Robert A. Pon, Rénald Gilbert, Anne Marcil, Risini D. Weeratna, and Scott McComb

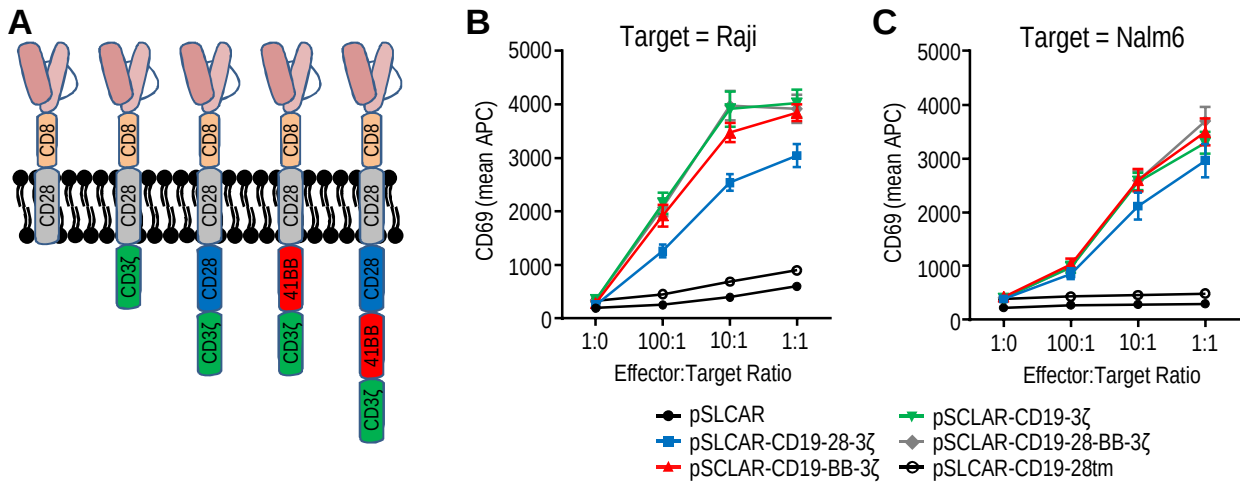

Figure S1: CAR-J does not robustly differentiate between signaling/co-stimulation domains for the anti-CD19 scFv derived from FMC63 (supplement to Figure 1).

(A) Depiction of CAR constructs containing different signaling/co-stimulation domains. (B) CAR-J dose-response when co-cultured with increasing numbers of CD19-positive Raji cells. (C) CAR-J dose-response when co-cultured with increasing numbers of CD19-positive Nalm6 cells. Results represent means +/- SEM of 3 independent experiments (n=3).

A

mAb clone	ELISA (OD at 405 nm)				Flow cytometry (MFI)	
	EGFRvIII protein		EGFR protein		U87-vIII	U87-MG
	Native	Denatured	Native	Denatured		
F260	1.736	1.743	0.001	0.000	4007	180
F263	1.527	0.997	1.698	0.001	3465[a]	175[a]
F265	0.874	0.623	0.002	0.000	2021	177
F269	1.125	0.517	0.011	0.001	2084	195
F271	0.935	1.054	0.004	0.000	1645	170
225	1.496	0.004	1.320	0.002	6574	11165
anti-GFP	-0.001	0.002	0.002	0.000	164	188

[a]performed with purified antibody

B

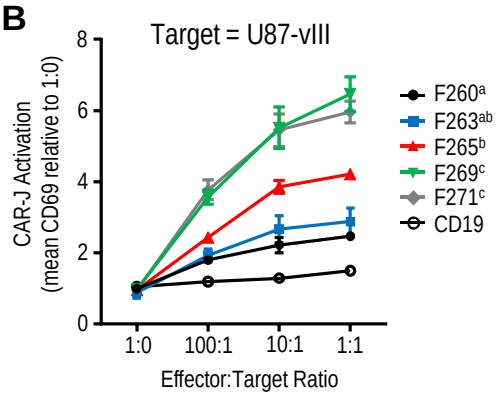

Figure S2: Characterization of novel anti-EGFRvIII mouse monoclonal antibodies (supplement to Figure 2). Monoclonal antibodies specific for the mutant form of EGFR (EGFRvIII) were generated using mouse immunization, hybridoma creation, and screening as described in the Methods section. (A) Monoclonal antibody characterization was then performed using indirect ELISA using purified mAbs (1 µg/ml). Antibodies were incubated with immobilized recombinant EGFRvIII or EGFR protein. Flow cytometry analyses using raw hybridoma supernatant was done on U87MG cell lines (wildtype U87 or EGFRvIII-expressing U87-vIII). Note that due to low IgG production from the hybridoma, flow cytometry analyses were performed using purified antibody for F263. Antibody 225 is a commercial anti-EGFR mAb that binds to a native epitope common to both EGFRvIII and EGFR which was used as a control antibody in these experiments. (B) Normalized data as presented in Figure 2C. Results in (B) represent means +/- SEM of 3 independent experiments (n=3). In (B), 1:1 ratio data was compared using 1-way ANOVA and significant differences are indicated with lower case letters, where groups with different letters are significantly different from each other.

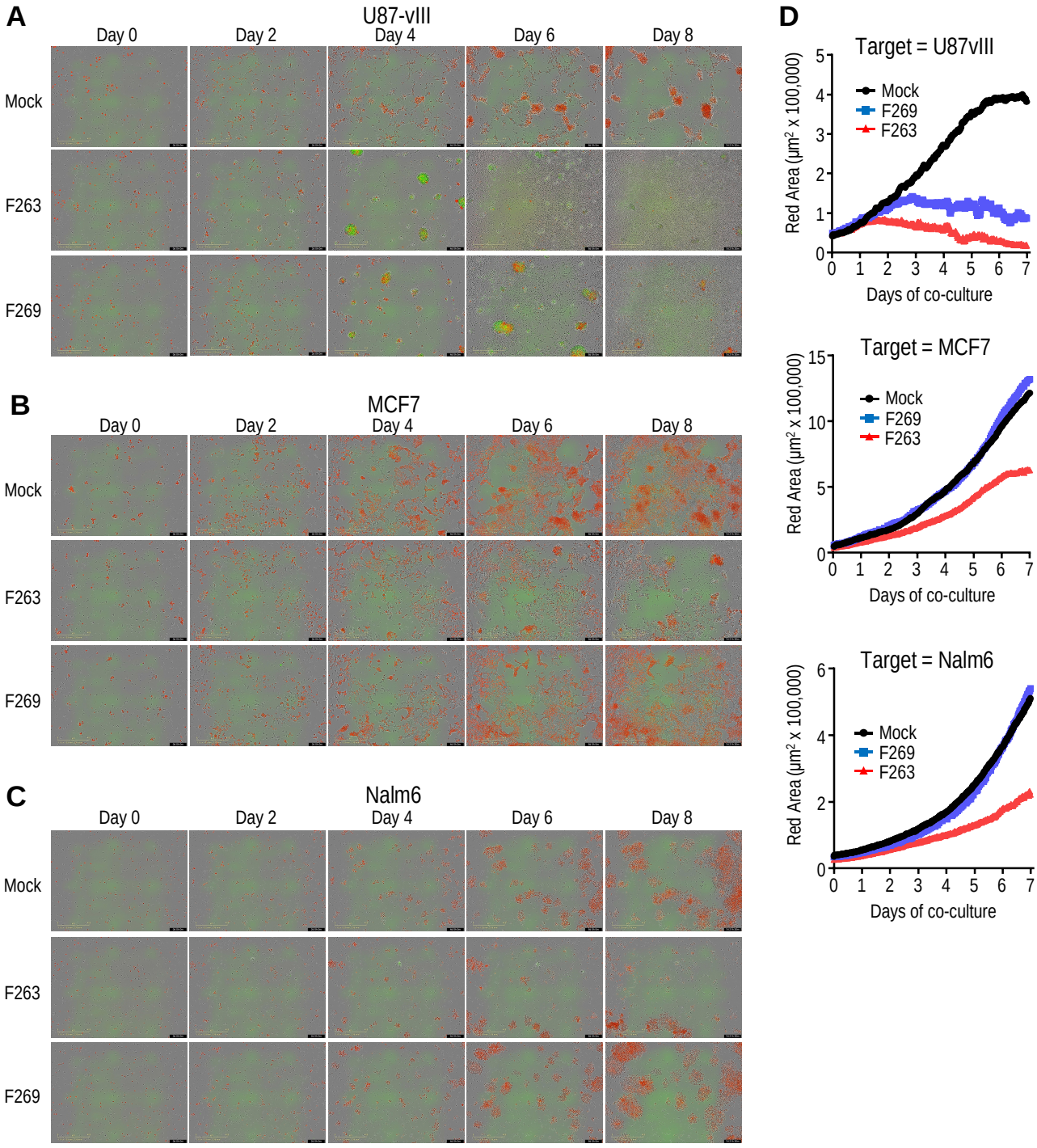

Figure S3: CAR-T effector function testing using continuous live-cell imaging: Donor 1 (supplement to Figure 4).

(A) Sample time-lapse images of mock (top) and F263 (middle) and F269 (bottom) EGFRvIII CAR-T cells (green) co-cultured at a 1:1 ratio alongside U87-vIII cells stably expressing nuclear-localized mKate2 (red). CAR-T activation and proliferation is apparent by formation of GFP-positive T cell blasts. (B) Similar sample images from MCF7 co-cultures. (C) Sample time-lapse images of mock (top) and F263 (middle) and F269 (bottom) EGFRvIII CAR-T cells (green) co-cultured at a 1:1 ratio alongside Nalm6 cells stably expressing nuclear-localized mKate2 (red). (D) Assessment of mKate2 (red) area measurements for co-cultures performed with CAR-T cells derived from Donor 1. These images correspond to Figure 5I & 5J.

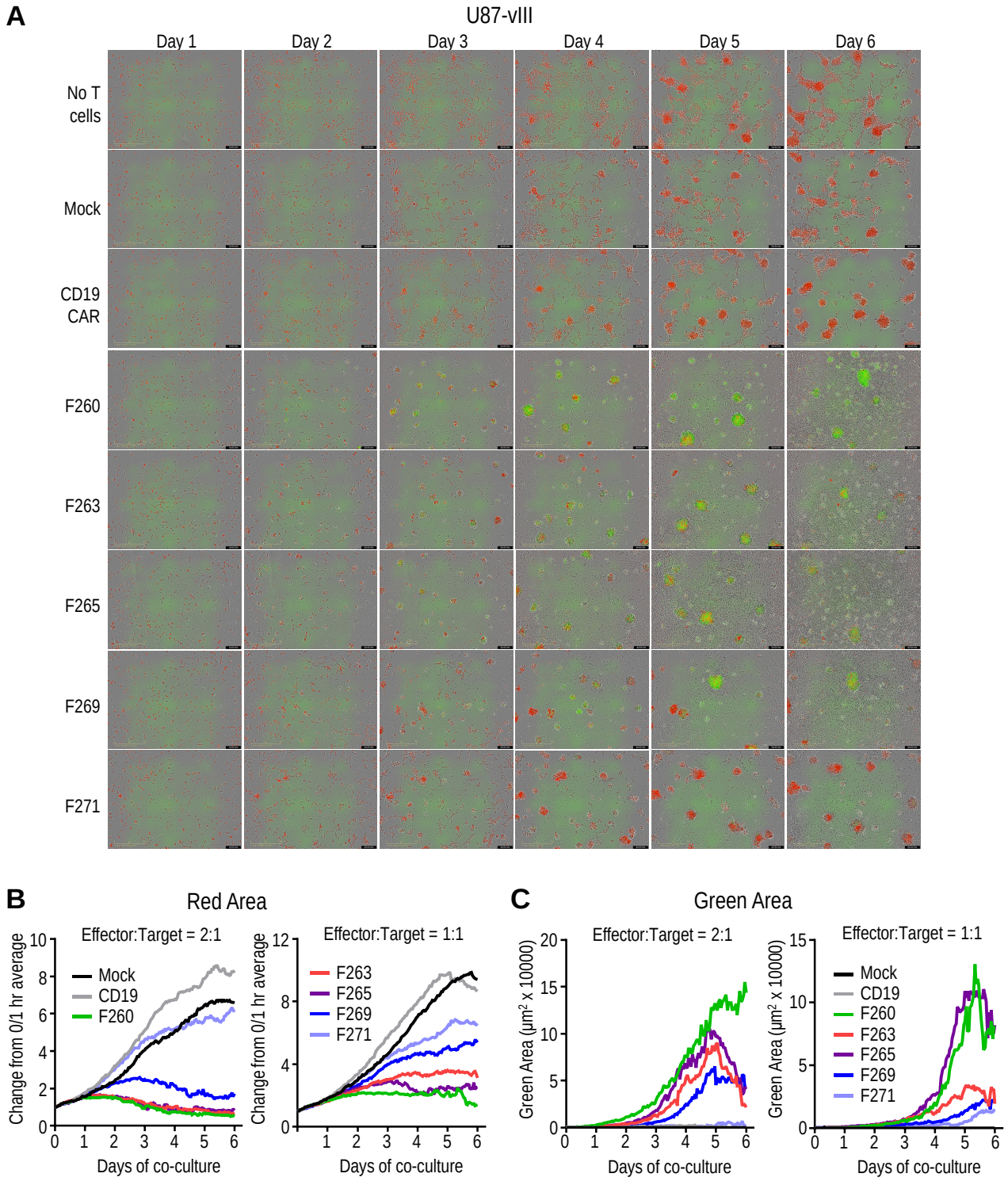

Figure S4: CAR-T effector function testing using continuous live-cell imaging: results from Donor 4 (supplement to Figure 4).

(A) Sample time-lapse images of EGFRvIII CAR-T cells (green) co-cultured at a 1:1 ratio alongside U87-vIII cells stably expressing nuclear-localized mKate2 (red). These images correspond to data reported in Figure 5I & 5J. Assessment of U87-vIII growth (mKate2 area) (B) and CAR-T proliferation (GFP area) (C) for Donor 4 co-cultures.

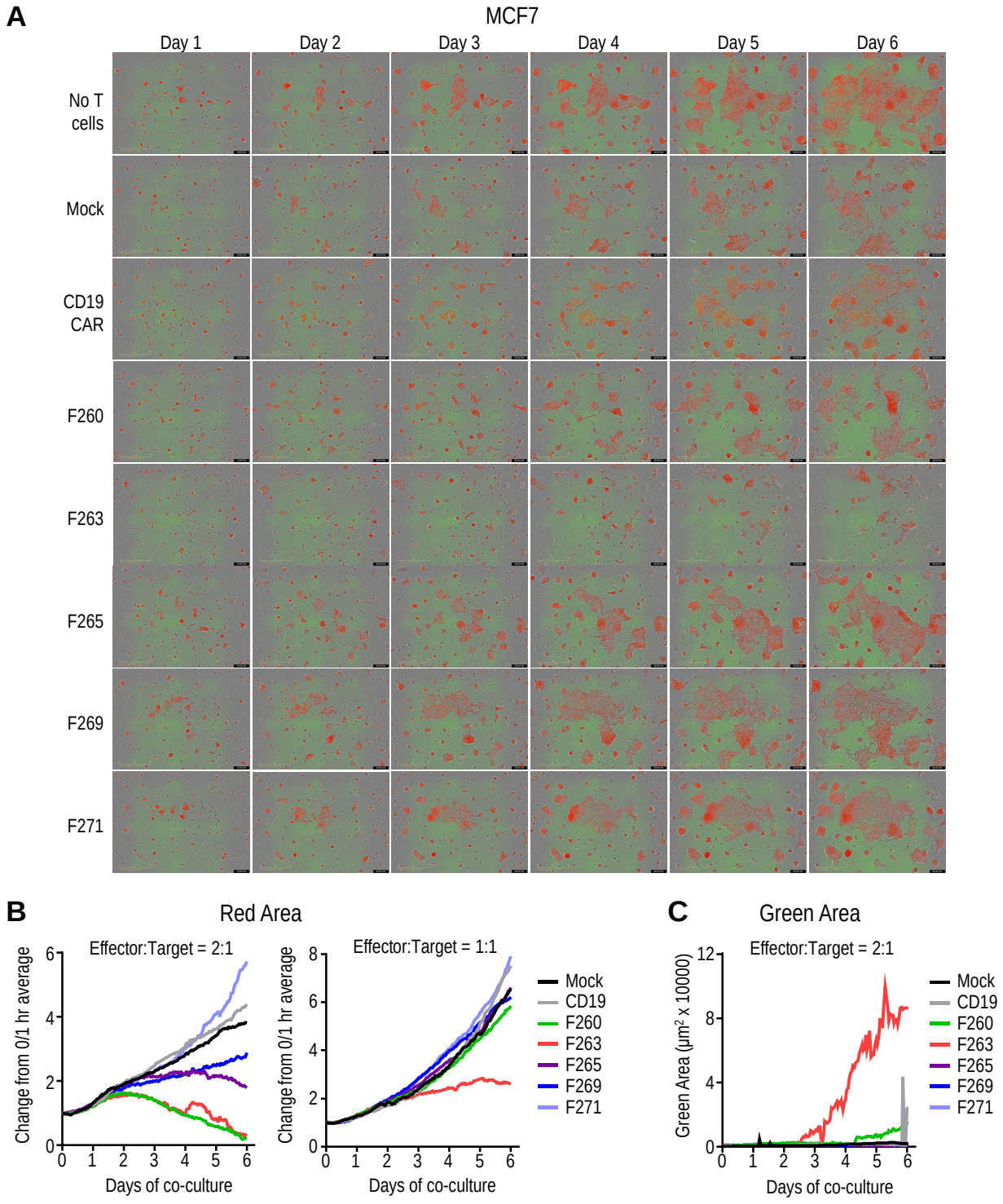

Figure S5. CAR-T effector function testing using continuous live-cell imaging: results from Donor 4 (supplement to Figure 4)

(A) Sample time-lapse images of EGFRvIII CAR-T cells (green) co-cultured at a 1:1 ratio alongside MCF7 cells stably expressing nuclear-localized mKate2 (red). These images correspond to Figure 5I & 5J. Assessment of MCF7 growth (mKate2 area) (B) and CAR-T proliferation (GFP area) (C) for Donor 4 co-cultures.

Day 0

Maintain healthy Jurkat and target cells.

Ensure adequate cell numbers by Day 2:
- 1 96-well plate = 4 x 10^6 Jurkat cells
- 1 96-well plate = 5 x 10^5 target cells

Ensure adequate pSLCAR-CD19 DNA:
- 16 wells = 600,000 Jurkat + 3 µg DNA per CAR construct being tested

Design and acquire target-specific scFv/ABD DNA sequences.

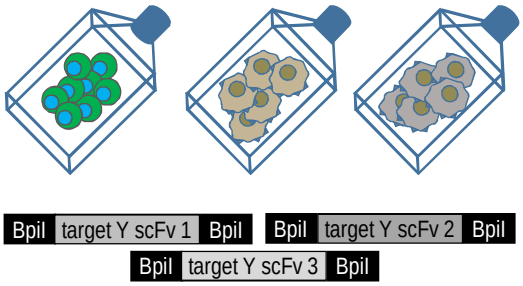

Day 1

Clone scFv/ABD DNA into pSLCAR-CD19 and transform into competent cells.

Alternate: use Gibson cloning.

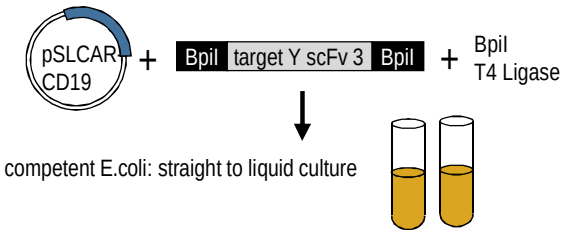

Day 2

Mini-prep polyclonal culture.

Perform CAR-J assay:
- Morning: electroporate Jurkat cells
- 4 hours later, co-culture with appropriate numbers of target cells.

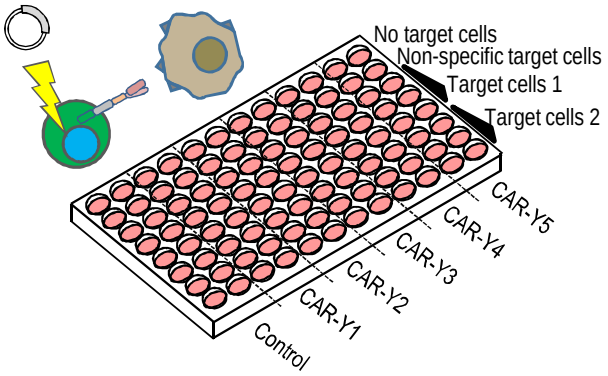

Day 3

Stain and analyze cells via flow cytometry.

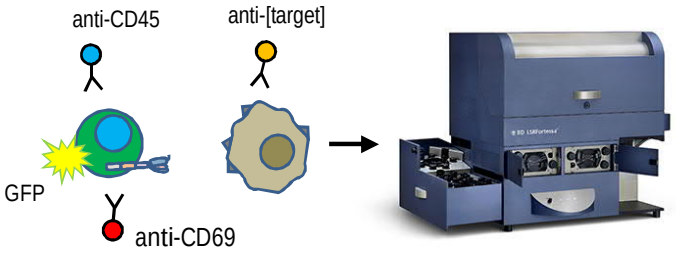

Figure S6. Overview of rapid CAR-J screening protocol. (supplement to Figure 6)

Supplemental Video Titles and Captions

Supplemental Video 1 (supplement to Figures 3-5): Time-lapse video created using live-cell images of Donor 4 non-transduced cells co-cultured with U87-vIII (red).

Supplemental Video 2 (supplement to Figures 3-5): Time-lapse video created using live-cell images of Donor 4 F263 CAR-T cells (green) co-cultured with U87-vIII (red).

Supplemental Video 3 (supplement to Figures 3-5): Time-lapse video created using live-cell images of Donor 4 F269 CAR-T cells (green) co-cultured with U87-vIII (red).

Supplemental Video 4 (supplement to Figures 3-5): Time-lapse video created using live-cell images of Donor 4 non-transduced cells co-cultured with MCF7 (red).

Supplemental Video 5 (supplement to Figures 3-5): Time-lapse video created using live-cell images of Donor 4 F263 CAR-T cells (green) co-cultured with MCF7 (red).

Supplemental Video 6 (supplement to Figures 3-5): Time-lapse video created using live-cell images of Donor 4 F269 CAR-T cells (green) co-cultured with MCF7 (red).